Paleo-Seismicity in the Euganean Hills Province (Northeast Italy): Constraints From Geomechanical and Geophysical Tests in the Schio-Vicenza Fault Area

Silvana Martin[1], Fabio Fedrizzi[2], Jacopo Boaga[1], Nicola Cenni[1], Claudia Agnini[1], Giampaolo Cortellazzo[3] and Sandro Rossato[4]*

[1]Department of Geosciences, University of Padova, Padua, Italy, [2]Geological Service of the Autonomous Province of Trento, Trento, Italy, [3]Department of Civil, Environmental and Architectural Engineering, University of Padova, Padua, Italy, [4]Institute of Geosciences and Earth Resources, National Research Council, Padua, Italy

Gouges and cataclasites within exhumed fault zones are valuable indicators of past seismic events. Gouge layers, 40- to 100-cm-thick and decameters long, have been found within uplifted Cretaceous limestones in the Euganean Hills (SW of Padova, NE Italy), Cenozoic subvolcanic chambers intruded within a Meso-Cenozoic sequence. The main tectonic lineament in the area is the Schio-Vicenza Fault that bounds the Euganean Hills to the East. Micropaleontological analyses reveal that the gouges derive from the fragmentation and pulverization of the adjacent pristine carbonatic rocks. Stress tests on specimens from bedrock associated with gouges yielded a minimum dissipated strain energy of 0.3–0.5 MJ/m^3 to shatter them. Henceforth, additional strain energy was necessary to pulverize these rocks within the gouge zones. Global navigation satellite system observations show that the present deformation pattern in this region of Italy is a few tens of nanostrain (10–30 1/y), not enough to generate such gouge layers. Therefore, the seismicity of the Euganean Hills (currently M ≤5) must be reconsidered in the light of the Schio-Vicenza Fault past activity. The gouges may imply that the Schio-Vicenza Fault had a more intense activity in the past, or this area was affected by remote events or tectonic structures. This article provides new clues on the evolution of the tectonic and morphological setting of the area, with relevant consequences on seismic risk assessment of the nearby urbanized area, including the cities of Padova and Vicenza.

Keywords: paleo-seismology, rock mechanic, Euganean Hills, Southern Alps, seismic hazard

INTRODUCTION

A territory hit by earthquakes generally exhibits distinctive landforms such as compressional and extensional features, ridges, shear planes with displacement, scarps, trenches and fragmented rocks, and gouges (powdered layers and pockets) within bedrock (i.e., Guerrieri et al., 2010; Michetti et al., 2012; Livio et al., 2014). These features have been observed in the central sector of the Italian Southern Alps (Vannoli et al., 2015). Before the recognition of paleo-seismic landforms indicative of earthquakes in the Southern Alps, it was generally accepted that no high-intensity seismic events,

with exception of the well-known earthquake of Verona in 1117, occurred in this area in the last millennia and many of the Middle Age city destructions in the NE Italy were attributed to this event (Guidoboni et al., 2005; Rovida et al., 2016). Actually, several lines of evidence of paleo-seismicity have been recognized so far. In the Como Lake area (**Figure 1**), pseudotachylite veins in the Grigne Group (Viganò et al., 2011), co-seismic turbiditic lacustrine sequences (Fanetti et al., 2008) and liquefaction features in Late Pleistocene deposits near Como indicate important past earthquakes (Chunga et al., 2007). Near Brescia (i.e., Mt. Netto), a spectacular ground rupture due to the growth of a decameter-scale fold in Pleistocene fluvioglacial sediments (Livio et al., 2009; Livio et al., 2014) and other paleo-seismic structures near the Garda Lake confirm strong past seismic events (Scardia et al., 2015). Highly fragmented to powdered rocks within Mesozoic carbonates along the Schio-Vicenza and Foiana faults (Fondriest et al., 2012; Fondriest et al., 2015; Fondriest et al., 2017; Viganò et al., 2018) are also interpreted as paleo-seismic evidence. Rock avalanche deposits in the Adige and Sarca valleys and Garda Lake area have been recently interpreted as a consequence of earthquakes possibly related to the Southern Giudicarie Fault (Martin et al., 2014; Ivy Ochs et al., 2017a; Ivy Ochs et al., 2017b). In the area between Bassano and

Pordenone, Miocene–Pliocene sequences have been deformed and uplifted in Pleistocene–Late Holocene due to the thrust activity of the Venetian-Friulian belt which was struck by earthquakes with magnitude M >5 (Galadini et al., 2005; Burrato et al., 2008; Fontana et al., 2010; Rovida et al., 2020). In the Po Plain, active blind thrusts and related transfer faults are present, and some of these are thought to act as potential triggers (i.e., Burrato et al., 2008; Vannoli et al., 2015).

The discovery of cataclasites and powdered layers and pockets in carbonatic lithologies cropping out in the Euganean Hills (SW Padova; **Figure 1**) has led to important different questions including 1a) were these gouge structures generated by paleo-seismic events? 1b) are the fragmented and powdered rocks derived through shattering and pulverization processes from the surrounding pristine rocks? 1c) are these fragmented and powdered rocks the result of one single event or are rather related to multiple successive episodes? 2) what is the minimum energy necessary to produce powdered layers and pockets from carbonatic lithologies and which is the strength drop of the rocks? 3) which fault or faults triggered this (these) paleo-seismic event(s) and why these structures and material are now exposed in the frontal part of the Euganean Hills?

FIGURE 1 | Map of the Southern Alps and the Po plain. The dashed rectangle shows the location of the Euganean Hills (**Figure 2**). Active faults (yellow and red lines) BV: Bassano-Valdobbiadene, RB: Riviera del Brenta (dashed line is the presumed continuation); SV: Schio-Vicenza. **Inset:** Alps with main lineaments; ESA: eastern Southern Alps thrust system; FPT: Frontal Penninic thrust; AST: Alpine Sole thrust; VS: Valsugana thrust; IL: Insubric Lineament. Background maps derive from a 20-m cell DTM (open data released by ISPRA: http://www.sinanet.isprambiente.it/it/sia-ispra/download-mais/dem20/view, last access: September 3, 2020).

In order to answer these questions, we collected both pristine rocks and the related powdered material from layers and pockets cropping out in the Euganean Hills and carried out micropaleontological, chemical, geomechanical, and geotechnical analyses. In the laboratory, we attempted to reproduce the damage observed in the field (shattering and pulverization) through static compression performed on samples loaded to failure. The measurement of the energy dissipated when breaking the rocks at the failure coincides with the peak stress, and it is proportional to the damage of the specimens in the laboratory. This can give us an approximate idea of the energy consumed by the friction to produce gouge during an earthquake (Scholz, 2020).

The results of these studies were integrated with seismic tests (seismic survey: measurement of compressional P-wave and shear S-wave velocities) in the southern part of the Euganean Hills to verify if other cataclasite and gouge layers were recognizable in the underground. The Euganean Hills belong to the Schio-Vicenza Fault area and are bordered to the east by a master fault. This area is characterized by earthquakes of magnitude 4< M <5 (Viganò et al., 2015; Guidoboni et al., 2018). By contrast, earthquakes with M >5 are widespread in the Venetian-Friulian thrust belt and related strike-slip faults (Viganò et al., 2015). The Euganean Hills can be considered part of this thrust belt even if it has been displaced to the south by the Schio-Vicenza Fault (**Figure 1**).

Past seismicity of the Euganean Hills is documented by few moderate magnitude earthquakes occurred in the Padova district (Guidoboni et al., 2007; Guidoboni et al., 2018) as for instance the earthquake recorded in 1491 (M = 5), which generated severe damage to the cultural heritage of the city. Understanding the paleo-seismic structures of the area could provide insights into paleo-events and related sources and would be helpful to verify if the sources are the same for both past and recent earthquakes, possibly allowing the forecast of the future event consequences.

All analyses performed in our research were integrated with both a geomorphological analysis of the Euganean landforms and a geodynamic scenario based on GNSS (global navigation satellite system) in order to provide a reliable assessment of the tectonic/ seismic risks of the study area. This approach helps constrain time, magnitude, and dynamics of prehistoric earthquakes and also provide important insights into the present seismic risk.

THE EUGANEAN HILLS

Tectonics and Magmatism

The Euganean Hills (~300 km^2, Padova Province, NE Italy) include a number of subvolcanic bodies of kilometric scale, belonging to the cluster of post-alpine magmatic intrusions within the Meso-Cenozoic carbonatic sequence (**Figure 1**). This magmatism followed the decoupling of the Northern and Southern Alps domains within the framework of late alpine geodynamic processes related to the indentation of the African Plate (Adria microplate) against Europe. At present, the African Plate underthrusts the European Plate below the Venetian-Friulian Prealps. In the Venetian Prealps, the shortening is

accommodated by S- to SE-vergent thrusts, the most important of which is the SE-verging Bassano-Valdobbiadene thrust (BV in **Figure 1**, Doglioni, 1992a; Doglioni, 1992b) which is interrupted by the NW-SE oriented Schio-Vicenza Fault (SV in **Figure 1**), which borders to the east the Lessini Mountains (N of Verona), the Berici (S of Vicenza), and Euganean Hills (SW of Padova).

The Schio-Vicenza is the principal fault of this area. Its activity influenced the intrusion and tectonic evolution of the Euganean Hills and controlled their seismicity (Pola et al., 2014). The main plane originated as a high-angle normal fault during the Paleogene or before in the Mesozoic and was subsequently reactivated since late Miocene as a sinistral strike-slip fault (Finetti, 1972; Castellarin et al., 2006; Zampieri et al., 2003; Galadini et al., 2004; D'Agostino et al., 2008; Serpelloni et al., 2016; Fondriest et al., 2012) joining the Southern Alps with the Adriatic coast over about 120 km. The fault was completely buried by sediments in the Venetian Plain and is not traceable at the surface (Antonelli at al., 1990; Vannoli et al., 2015). His occurrence is indicated by seismic sections across the fault area including minor faults subparallel to the master fault (see **Figure 5** in Pola et al., 2014; **Figure 1**). At Abano Terme, a small town near the Euganean Hills, buried extensional structures sealed by hydrothermal sediments suggest this fault was active ~34 ka ago (Pola et al., 2014; Torresan et al., 2020). The Euganean Hills are elongated in an NNW-SSE direction between Bastia to the north and Monselice to the south (**Figure 2A**). Northward, the Euganean Hills are separated from the Berici Hills by the NE-SW–oriented Riviera dei Berici fault (RB in **Figure 1**; Piccoli et al., 1976; Antonelli et al., 1990) which played a very important role separating the Berici shallow sea setting from the Euganean pelagic domain. An NE-SW structural high is reported to be active from late Campanian to early Eocene across the Euganean Hills, separating the northern condensed sequences present in the Berici Hills from the northern Euganean Hills which instead show thicker sequences and enhanced terrigenous input with respect to the southern part of the Euganean Hills (Massari and Medizza, 1973). Other N-S, NW-SE, and E-W trending faults have been active almost since the early Oligocene, as indicated by the direction of the magmatic dykes, in an extensional tectonics scenario (Piccoli et al., 1976; Pola et al., 2014). Forty kilometer south of the Euganean Hills, the fold-and-thrust belt of the Northern Apennines, growing up since the Late Cretaceous, moved northward while deforming the Pliocene-Pleistocene sedimentary sequence of the Po Plain (Doglioni, 1993; Carminati et al., 2010; Govoni et al., 2014) (**Figure 1**).

The Euganean Hills derived from a single magmatic apparatus alimented by the Mt. Venda magmatic center in the area between the Schio-Vicenza and Riviera dei Berici faults (**Figures 1, 2**), suggesting a correlation between the tectonic and magmatic activity in the middle Eocene to early Oligocene time (Dieni and Proto Decima, 1970; Cucato et al., 2011; Cucato et al., 2012; Bartoli et al., 2015). Intrusions at a depth of around 8–10 km (Piccoli et al., 1976; Piccoli et al., 1981; Zaia et al., 1989) produced a first uplift of the Euganean crust followed by an erosional phase. After the cooling at a shallower depth, between 23 and 21 million years ago ((U-Th)/He apatite fission tracks data; Benà et al.,

2019), the magmatic rocks have been brittle deformed. These intrusions are now exposed reaching a maximum elevation of 603 m (i.e., Mt. Venda) and looking like pyramidal volcanoes. The most known bodies, besides the Mt. Venda edifice, are located in the northern part, near the village of Teolo (i.e., Mt. Madonna and Mt. Grande), and in the southern part, near the village of Arquà Petrarca (i.e., Mt. Orbieso, Mt. Ventolone, and Mt. Ricco). Three samples of magmatic rocks were collected from dykes all over the area (rhyolite VP6, andesite VP15, and perlite AP17; **Figures 2B,C**; **Table 1**). At the slopes of these hills, the Maiolica (Upper Jurassic–Lower Cretaceous), Scaglia Variegata Alpina (Cretaceous), Scaglia Rossa (Upper Cretaceous-middle Eocene), and Torreglia Formation (upper Eocene–lower Oligocene) crop out (De Zigno, 1861; Massari and Medizza, 1973; Piccoli et al., 1976; Piccoli et al., 1981).

Lithostratigraphy

The area between Arquà Petrarca and Teolo is a kilometric-scale wide anticline with an ENE-WSW trending axis, parallel to the undulations of the Berici Hills and eastern Lessini Mountains (Piccoli et al., 1976). The adjacent syncline is located close to the village of Teolo (**Figure 2A**). The lithostratigraphic units cropping out in this area are the following (**Figure 2A**):

1) Maiolica (Tithonian pp.–Aptian). This unit is a white, light gray micritic limestone with black chert lenses, with a maximum thickness of ~80–90 m; in the study area, it is strongly reduced if compared with the Venetian Prealps area (Astolfi and Colombara, 2003). Maiolica gradually transforms locally into the overlying Scaglia Variegata Alpina, but the contact between these two lithologic units are not always easily distinguishable. The most common microfossils found in Maiolica are calcareous nannofossils (Piccoli et al., 1976). Maiolica intact samples and gouges were collected north of the village of Arquà Petrarca (Val Pomaro: rock samples VP10, VP10bis, VP23, VP24, VP25, and VP26 and gouges VP9 and VP14; **Figure 2C**) and near the village of Teolo (rock samples: T13A-B, T14A-B; **Figure 2B**).

2) Scaglia Variegata Alpina (Aptian–Cenomanian). This unit is a micritic limestone white in color with black or red chert lenses lying on the top of Maiolica. The thickness is about 40–45 m. Bedding is thin, with plane joints and frequent stylolites. Locally, these rocks are composed of dark bituminous limestone; the boundary with the underlying Maiolica is globally characterized by Oceanic Anoxic Event 2, which is locally referred to as the Bonarelli event (Jenkyns, 2010). This unit crops out near Teolo (Cucato et al., 2011).

3) Scaglia Rossa (Turonian–Lutetian). This unit is a reddish and marly limestone; whitish/pinkish lithologies with red–brown–green chert lenses are typical of the southern part of the Euganean Hills. The thickness varies from 80 m in the north to 130 m in the south. The Scaglia Rossa is divided into two informal members: the lower one is mostly carbonatic with thicker layering (Scaglia Rossa 1; **Table 1**) and the upper one is generally more marly (Scaglia Rossa 2;

Table 1) and is characterized by the presence of two hardgrounds of late Campanian-Maastrichtian age (Massari et al., 1976). Scaglia Rossa with very high clay content crops out in the southern part of the Euganean Hills and has an estimated age of early Eocene (Cucato et al., 2011). The decameter- to meter-scale folds present in the Scaglia Rossa were interpreted as being due to submarine slumping (Piccoli et al., 1976). Over the Scaglia Rossa, the sequence includes the clay-rich Torreglia formation, typical of basinal conditions of middle Eocene–early Oligocene age (Massari et al., 1976; Cucato et al., 2011). The thickness of the Eocene–Oligocene sequence, including the upper portion of Scaglia Rossa and the Torreglia Formation, is of ~1,000 m (Piccoli et al., 1976).

In the southern part of the Euganean Hills, near Arquà Petrarca, discontinuous whitish, few tens of meters long and 0.4- to 1-m-thick powdered layers of gouge and whitish pockets occur within Scaglia Rossa and Maiolica. Similarly, in the northern part of the Euganean Hills near Teolo, a discontinuous white-colored gouge layer few tens of meters long and 1 m thick occurs within Scaglia Rossa. In these sites, the decametric slumping and synsedimentary structures are tectonically reactivated. The Scaglia Rossa samples were collected at different sites (**Table 1** and **Figures 2B,C**): Mt. Bignago (rock: samples AP3, AP20, and AP28 from the side of the road and a quarry; samples AP29 and AP30 from the northern side of this hill; cataclasite AP1 and gouge AP4 from the side of the road), Mt. Mottolone (VP18), near the villages of Baone (AP32), and Teolo (rock T4 and gouges T1, T12).

Geomorphology

The Euganean Hills are considered as the product of subaerial erosion starting with the Miocene marine regression which exposed laccolites and dykes (Pellegrini, 1988; Pellegrini, 2006). Some weakly dipping morphological surfaces preserved at different altitudes were interpreted by Schlarb (1961) as remnants of relict surfaces due to different erosive cycles, after various uplift episodes of the hills, each one followed by a stability phase with smoothing (Reyer, 1877; Pellegrini, 2006). The uplift of the hills is indicated by valleys deeply incised and oversized with respect to their creeks (De Marchi, 1905; De Marchi, 1935). The uplift of the hills is suggested by the paleo-wandering of the Brenta River to the east and of the Adige River to the south (Nicolis, 1898). During Pleistocene, the Adige and Brenta rivers provided sediments which completely buried the foot of the Euganean Hills and overflooded some of the internal valleys (Castiglioni, 1982a; Castiglioni, 1982b; Castiglioni et al., 1987; Marcolongo and Zaffanella, 1987; Castiglioni and Pellegrini, 2001; Mozzi, 2001; Mozzi et al., 2010; Mozzi et al., 2013). To the east of the Euganean Hills, the Brenta River was recognized to have flown along three different main paths, which point out its migration from west to east since the middle Holocene (Castiglioni, 1982a; Castiglioni, 1982b; Fontana et al., 2014). Similarly, the Adige River migrated from north to south in an interval spanning from the Late Bronze Age to the High Middle Ages (II millennia BC and VII–VIII century AD; Ferrari et al., 2009; Piovan et al., 2010; Piovan et al., 2012).

TABLE 1 | Samples from the Euganean Hills. Rock type and geomechanical and geotechnical characteristics are reported.

| Sample	Location	Material	Latitude north WGS84	Longitude east WGS84	Classification USCS	Liquidity limit (%)	Plasticity index (%)	Residual shear strength φ (°)	Ring test	Uniaxial test σ_1 (MPa)	Triaxial test σ_1; σ_3 (MPa)	Indirect tensile strength [MPa]
VP6	Mt. Venda	Rhyolite dyke	45°17'98.9''	11°42'17.0''						49.5		
VP9	Val Pomaro: Gouge layer	Maiolica (Tithonian-Aptian)	45°16'37.0''	1°42'38.1''	ML	34	5					
VP10	Val Pomaro	Maiolica (Tithonian-Aptian)	45°16'38.3''	11°42'34.9''						28.7		
VP10bis	Val Pomaro	Maiolica (Tithonian-Aptian)	45°16'38.3''	11°42'34.9''								
VP14	Val Pomaro: Cataclasite pocket	Maiolica	45°16'24.9''	11°42'52.4''	ML	44	9					
VP15	Val Pomaro	Andesite dyke	45°16'24.4''	11°42'53.8''						38.5		
VP18	Mt. Mottolone	Scaglia Rossa 2 (upper Ypresian)	45°16'50.0''	11°42'21.3''							33.9; 3.0	
VP23	Val Pomaro	Maiolica (Tithonian-Aptian)	45°16'36.6''	11°42'41.5''								11.658; 6.701
VP24	Val Pomaro	Maiolica	45°16'36.6''	11°42'41.5''								4.797
VP25	Val Pomaro	Maiolica	45°16'29.2''	11°42'48.2''								6.806
VP26	Val Pomaro	Maiolica	45°16'29.2''	11°42'48.2''								13.236
AP1	Mt. Bignago: Cataclasite below the synsedimentary fold at the border of the quarry	Scaglia Rossa 1 (Upper Cretaceous)	45°15'26.1''	11°42'54.9''	ML	37	9	34.7	x			
AP3	Mt. Bignago: Main outcrop along the road. From a fold over the gouge layer (AP4)	Scaglia Rossa 1 (Upper Cretaceous)	45°15'30.0''	11°42'51.6''								
AP4	Mt. Bignago: Main outcrop along the road. Gouge layer	Scaglia Rossa 1 (Upper Cretaceous)	45°15'30.0''	11°42'51.6''	ML	42	12	35.0	x			
AP17	Mt. Ricco	Perlite dyke	45°15'28.3''	11°43'52.9''						113.0		
AP20	Mt. Bignago: The quarry	Scaglia Rossa 1 (Santonian-Campanian)	45°15'28.7''	11°42'53.8''						105.6		
AP28	Mt. Bignago: Top of the quarry	Scaglia Rossa 1 (Santonian-Campanian)	45°15'26.1''	11°42'54.9''								8.167
AP29	Mt. Bignago: Top of the hill, northern side	Scaglia Rossa 2 (Santonian-Campanian)	45°15'32.2''	11°42'51.3''						22.8		
AP30	Mt. Bignago: Top of the hill, northern side	Scaglia Rossa 2 (Santonian-Campanian)	45°15'32.2''	11°42'51.3''							66.9; 5.0	
AP32	Baone	Scaglia Rossa 1 (Santonian-Campanian)	45°15'40.5''	11°41'08.2''								4.117; 5.343
T1	Teolo: Gouge over cataclasite	Scaglia Rossa 1	45°20'53.9''	11°40'55.6''	SM	38	6	35.0	x			
T4A	Teolo: Block in cohesive cataclasite	Scaglia Rossa 1	45°20'53.9''	11°40'55.6''	—						167.8; 8.0	5.945; 5.099
T4B	Idem	Scaglia Rossa 1	45°20'53.9''	11°40'55.6''	—							3.557
T12	Teolo: Gouge over cataclasite	Scaglia Rossa 1	45°20'53.9''	11°40'55.6''	ML	28	4	34.5	x			
T13A-A	Villa di Teolo	Maiolica	45°20'28.6''	11°41'14.1''							143.0; 8.0	
T13A-B	Idem	Maiolica	45°20'28.6''	11°41'14.1''						97.0		
T14A	Villa di Teolo	Maiolica	45°20'46.1''	11°40'59.9''						169.9		
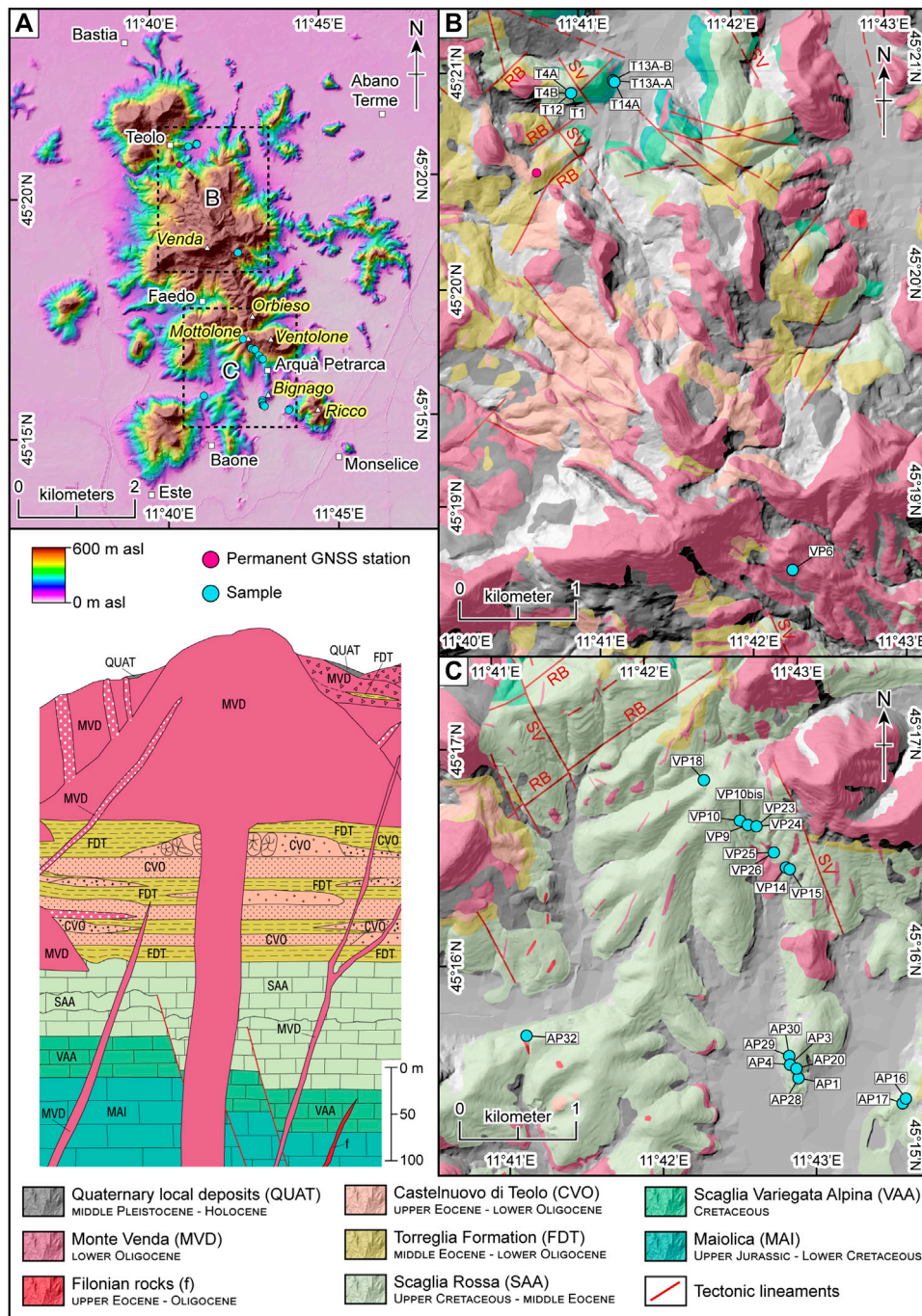
FIGURE 2 | Maps of the Euganean Hills with permanent GNSS (Global Navigation Satellite System) station (red) and sampling sites (light blue). Names of the locations are bordered in white if referring to towns and in yellow if referring to peaks. Samples: VP from Val Pomaro, AP from Arquà Petrarca, Mt. Bignago and Baone, and T from Teolo. The lithologies, the tectonic lineaments, and the stratigraphic sketch are modified from Cucato et al. (2011). Faults (red lines): RB Riviera del Brenta and SV Schio-Vicenza faults. Background maps derive from a 5-m cell DTM (open data released by Regione Veneto: http://idt.regione.veneto.it/app/metacatalog/, last access: September 3, 2020). **A**: general frame; **B**: northern Euganean Hills; **C**: southern Euganean Hills.
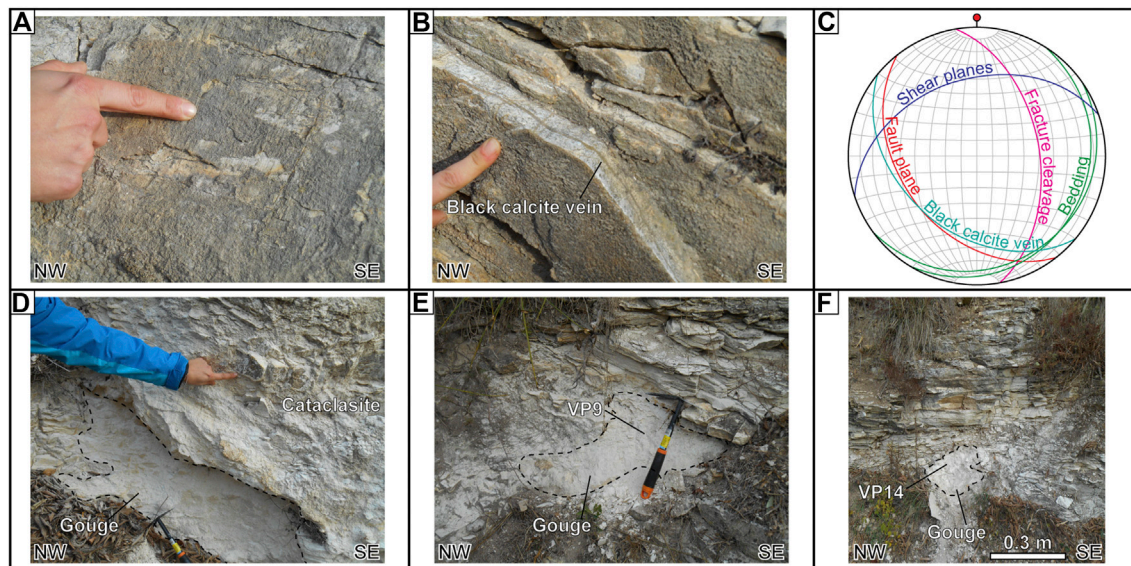
FIGURE 3 | Photographs and stereographic plot from Val Pomaro outcrops of Maiolica (coordinates: N45°16′38.3′′ E11°42′34.9′′; site 4 in **Supplementary Material 1**). For the location of the cited samples refer to **Figure 2C**. **A**: normal fault and striae along SW-dipping fault plane; **B**: SW-dipping fault vein filled with black calcite; **C**: stereoplot of collected data (NE-SW trending bedding, NW-trending fault plane, ENE-trending shear plane, N-S trending fracture plane, and NW-trending black calcite vein); **D**: cataclasite and underlying gouge pocket in Maiolica; **E**: gouge VP9; **F**: gouge VP14.

METHODS

Field Survey

Field surveys consisted of direct observation of the outcrops at different sites of the Euganean Hills. Three of these, Val Pomaro and Mount Bignago near Arquà Petrarca to the south and Teolo to the northeast, were selected for collecting structural data and rock and powdered samples for laboratory analyses.

Val Pomaro

A few kilometers north of Arquà Petrarca, in Val Pomaro (**Figure 2**), Maiolica is intruded by the trachyte laccoliths of Mt. Orbieso (326 m a.s.l.) and Mt. Ventolone (408 m a.s.l.). On the western flank of these hills, the sedimentary formations are plunging to the west (**Figure 2A**; see sites 2, 3 in **Supplementary Material 1**). Here, an NW-SE–oriented fault borders the laccoliths to the west and cuts Maiolica (**Figures 3A,C**). This fault dislocates the NE-SW–oriented faults of the Riviera del Brenta system. According to Piccoli et al. (1976), in many places, slices of Maiolica have been moved from the underground to the surface by the magmatic intrusions. Quaternary cover on the top of the outcrop is ~30 cm thick.

In upper Val Pomaro, the Maiolica bedding is 144/15–120/19 (dip direction/dip) (**Figure 2A**; site 4, map in **Supplementary Material 1**). Near the Val Pomaro restaurant, Maiolica is cut across by a normal fault with a plane dipping of 220/40 (photograph A and stereoplot C in **Figure 3**). Black calcite veins with a similar orientation (photograph B in **Figure 3**) and NNW-dipping shear planes (stereoplot C in **Figure 3**) are also present. Other NNW-

dipping shear planes were measured near Arquà Petrarca (site 3, map and plot in **Supplementary Material 1**). Maiolica is characterized by the presence of cataclasite and gouge layers and pockets reaching a maximum length and width of 3 and 1.5 m, respectively (photograph D in **Figure 3**). The gouge (VP9) and the relative pristine rock (VP10 and VP10bis) were collected from, and close to, a pocket about 0.80 m long and 0.30 m high (photograph E in **Figure 3**). The transition from cataclasite to powder in the layers and in the pockets is gradual. The gouge appeared compact, but it crumbled easily when touched. This material also forms the silt matrix of the associated cataclasite. Other Maiolica samples (VP23, VP24, VP25, and VP26) and the gouge (VP14) were collected along the road bound for Arquà Petrarca (photograph F in **Figure 3**; sites 4, 5 in **Supplementary Material 1**). Rocks and gouges were classified as Maiolica on the base of micropaleontological analyses (**Supplementary Material 2**), while in the geological map, the indicated lithology is Scaglia Rossa (Cucato et al., 2011).

Mt. Bignago

At Mt. Bignago, ca. 1 km south of Arquà Petrarca, an abandoned quarry (i.e., the Contarine quarry, 50 m a.s.l) excavated in the Scaglia Rossa is present (**Figure 2**; site 7, map and plot in **Supplementary Material 1**). Here, Scaglia Rossa has a high carbonate content, with rare clayey interlayers. It includes red chert lenses and bands deformed by metric to decametric isoclinal-like folds interpreted as synsedimentary (Massari and Medizza, 1973). The bedding in the quarry is N- to NW-dipping, but it is strongly altered by
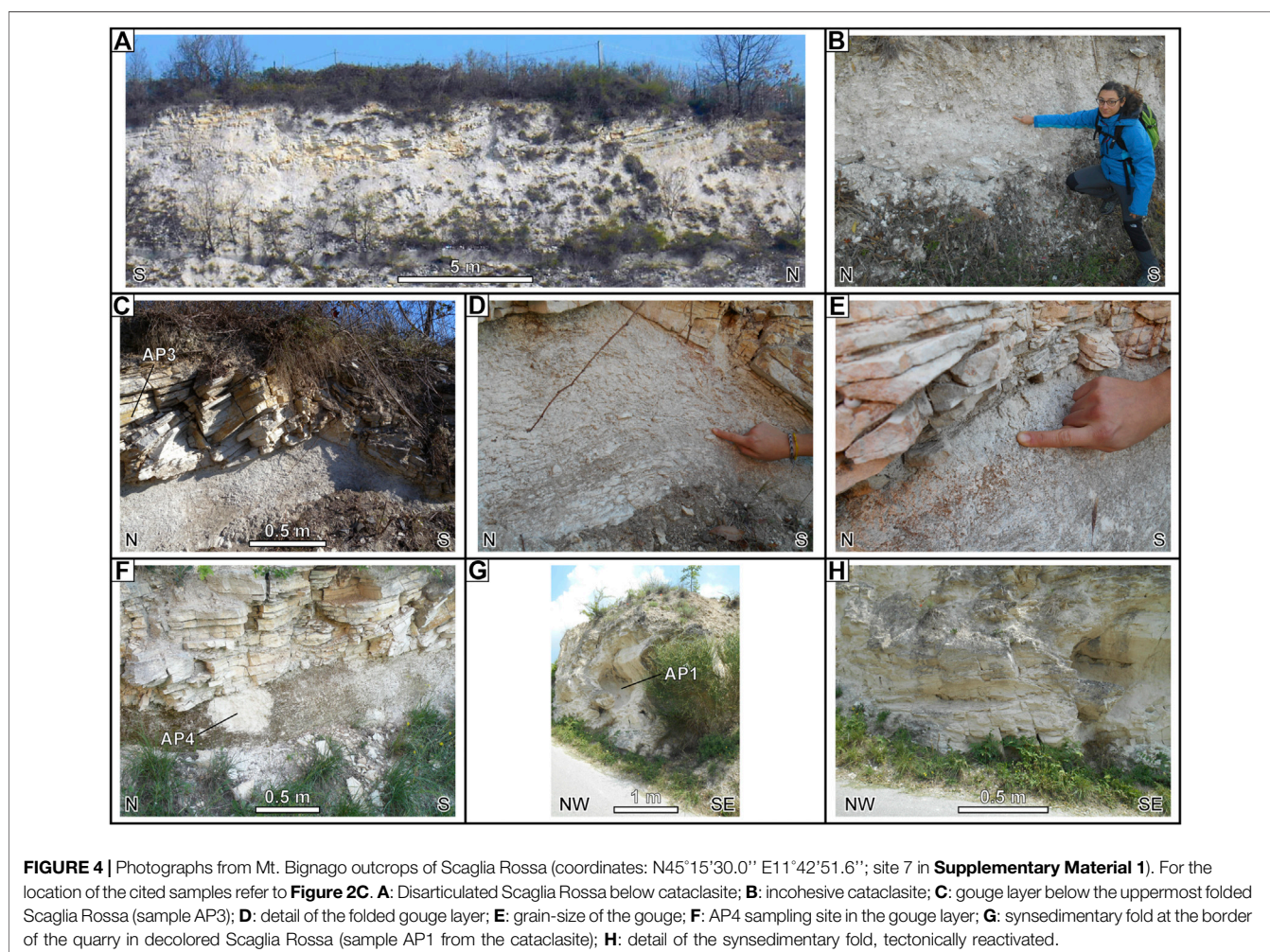
N-dipping shear planes. In the upper part of the quarry (photograph A in **Figure 4**), from bottom to top, we observe the following:
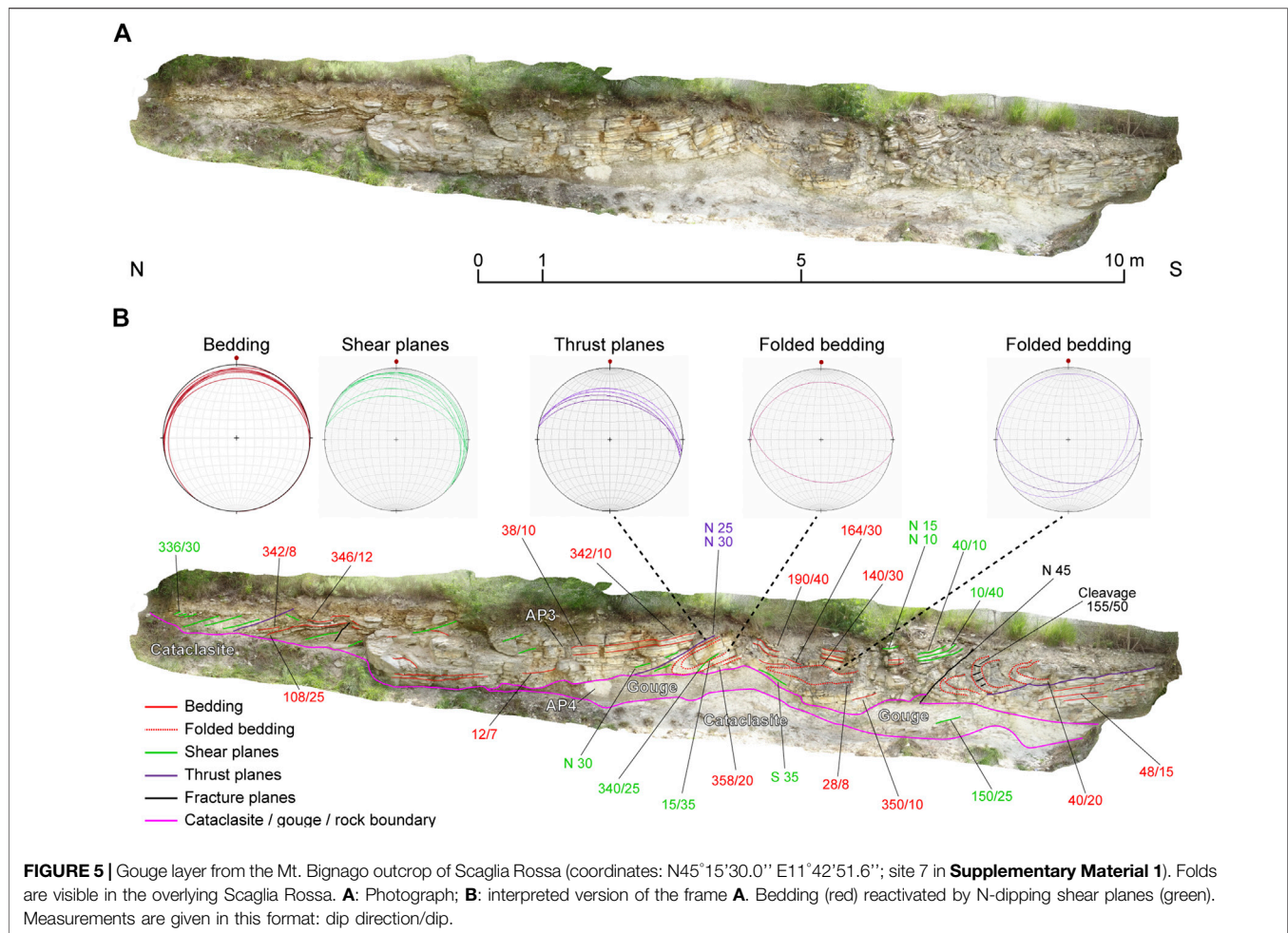
- a 5-m-thick pack of strata ascribable to Scaglia Rossa that is strongly fragmented and chaotically assembled in a cataclastic, clay-rich matrix (photograph A in **Figure 4**);
- a 2-m-thick cataclasite, cropping out also along the Mt. Bignago road over the quarry (photograph B in **Figure 5**);
- a 0.5- to 1-m-thick flour-like white gouge layer that is 30 m long where sample AP4 was collected (photographs C, D, E, and F in **Figure 4**);
- a strongly foliated and folded Scaglia Rossa at the top of the quarry where sample AP3 was collected (**Figure 2C**; photograph C in **Figure 4**).

One of the isoclinal-like folds observed in Scaglia Rossa over the gouge layer has the axis oriented N310/10 (for details, see Via Bignago, site a, in **Supplementary Material 1**). Another fold shows a typical fracture cleavage. The overlying folded Scaglia Rossa, the gouge layer, and cataclasites are weakly undulated (photographs C and D in **Figure 4**). The gouge layer composed of flour-like material is zoned and consists of two sublayers: the external layer (~0.2 m thick) is composed of randomly arranged material, while the internal layer (~0.8 m thick) preserves the original bedding (photograph E in **Figure 4**). The flour-like material of the external sublayer is composed of very fine grain size and has been classified as silt (see paragraph Gouges). The gouge has the same biostratigraphic age, based on calcareous nannofossils, of the overlying Scaglia Rossa (**Supplementary Material 2**). The gouge shows a static setting, without fluidification or slip, but it is weakly folded with E-W axis together with the overlying pristine Scaglia Rossa (**Figure 5**). The site is absolutely dry.

At the southern border of the quarry, a decametric synsedimentary fold, similar to others observed here, has been recognized (photograph G in **Figure 4**). This fold has been reactivated by shear deformation, resulting in the development of a south-vergent asymmetric setting and C-planes (photograph H in **Figure 4**; stereoplots of Via Bignago, site b, in **Supplementary Material 1**). The cataclasite sample AP1 was collected below the hinge of this tectonically reactivated synsedimentary fold.

FIGURE 4 | Photographs from Mt. Bignago outcrops of Scaglia Rossa (coordinates: N45°15'30.0'' E11°42'51.6''; site 7 in **Supplementary Material 1**). For the location of the cited samples refer to **Figure 2C**. **A**: Disarticulated Scaglia Rossa below cataclasite; **B**: incohesive cataclasite; **C**: gouge layer below the uppermost folded Scaglia Rossa (sample AP3); **D**: detail of the folded gouge layer; **E**: grain-size of the gouge; **F**: AP4 sampling site in the gouge layer; **G**: synsedimentary fold at the border of the quarry in decolored Scaglia Rossa (sample AP1 from the cataclasite); **H**: detail of the synsedimentary fold, tectonically reactivated.

FIGURE 5 | Gouge layer from the Mt. Bignago outcrop of Scaglia Rossa (coordinates: N45°15'30.0'' E11°42'51.6''; site 7 in **Supplementary Material 1**). Folds are visible in the overlying Scaglia Rossa. **A**: Photograph; **B**: interpreted version of the frame **A**. Bedding (red) reactivated by N-dipping shear planes (green). Measurements are given in this format: dip direction/dip.

Slumping and synsedimentary deformation are common in the Mt. Bignago Scaglia Rossa of Campanian age (planktonic foraminifera *Globotruncanita elevata* zone; see Piccoli et al., 1976, *p*. 187). In the Euganean and Berici hills, the synsedimentary fold axes are consistent with the Schio-Vicenza Fault paleoactivity (slumping fold axes oriented N70 E were measured in the Cretaceous olistostrome enclosed in the middle Eocene marly limestone in the Berici Hills; Piccoli et al., 1976). Slumping and synsedimentary folding are indicative of a tectonic instability during Cretaceous and Eocene (Piccoli et al., 1976, *p*. 186), but a tectonic reactivation of this fault occurred during a successive activity phase. A drilling in the valley to the north of Mt. Bignago confirms the presence of strongly fragmented and disarticulated Scaglia Rossa below 40 m of peat and alluvial material (Cucato et al., 2012); this datum is consistent with the observation made in the quarry. The Quaternary cover on top of Mt. Bignago is about 0.3 m thick.

Samples were collected from pristine Scaglia Rossa and powdered layers (see **Figure 2C** for locations) to demonstrate that they are composed of the same material based on micropaleontological content (**Supplementary Material 2**). Rock (AP3), cataclasite (AP1), and gouge (AP4) samples have a similar chemical and mineralogical compositions (see **Supplementary Material 3** for

chemistry and **Supplementary Material 4** for mineralogy data). These samples have a high carbonate content and consist of dominant calcite with the presence of quartz, white mica, and clay; the gouge sample (AP4) is the richest in nontronite (Figures 1A,B in **Supplementary Material 4**). Scaglia Rossa sample (AP20), coming from the upper part of the Mt. Bignago quarry, has a high carbonate content as sample AP3. On the contrary, samples collected from the top of the Mt. Bignago in the northern side (AP28, AP29, and AP30) and from Mt. Mottolone (VP18) are clay enriched.

Teolo

In the northeastern part of the Euganean Hills, approximately 1 km east of Teolo (70–80 m a.s.l.), a 30-m-long gouge layer is present within Scaglia Rossa (**Figures 2A,B, 6**). The Teolo valley is oriented about ENE-WSW, parallel to a weak anticline followed to the northwest by the Teolo syncline; the base of the succession is composed of subhorizontal not typical Maiolica which is characterized by a higher amount of clay and the presence of bituminous black sediments, overlying Scaglia Rossa and Torreglia formation (middle-upper Eocene).

At the southwestern end of the valley, the Rocca Pendice trachyte dyke (Rocca Pendice peak is at an elevation of 320 m a.s.l.) cuts across the western limb of the Teolo syncline. The
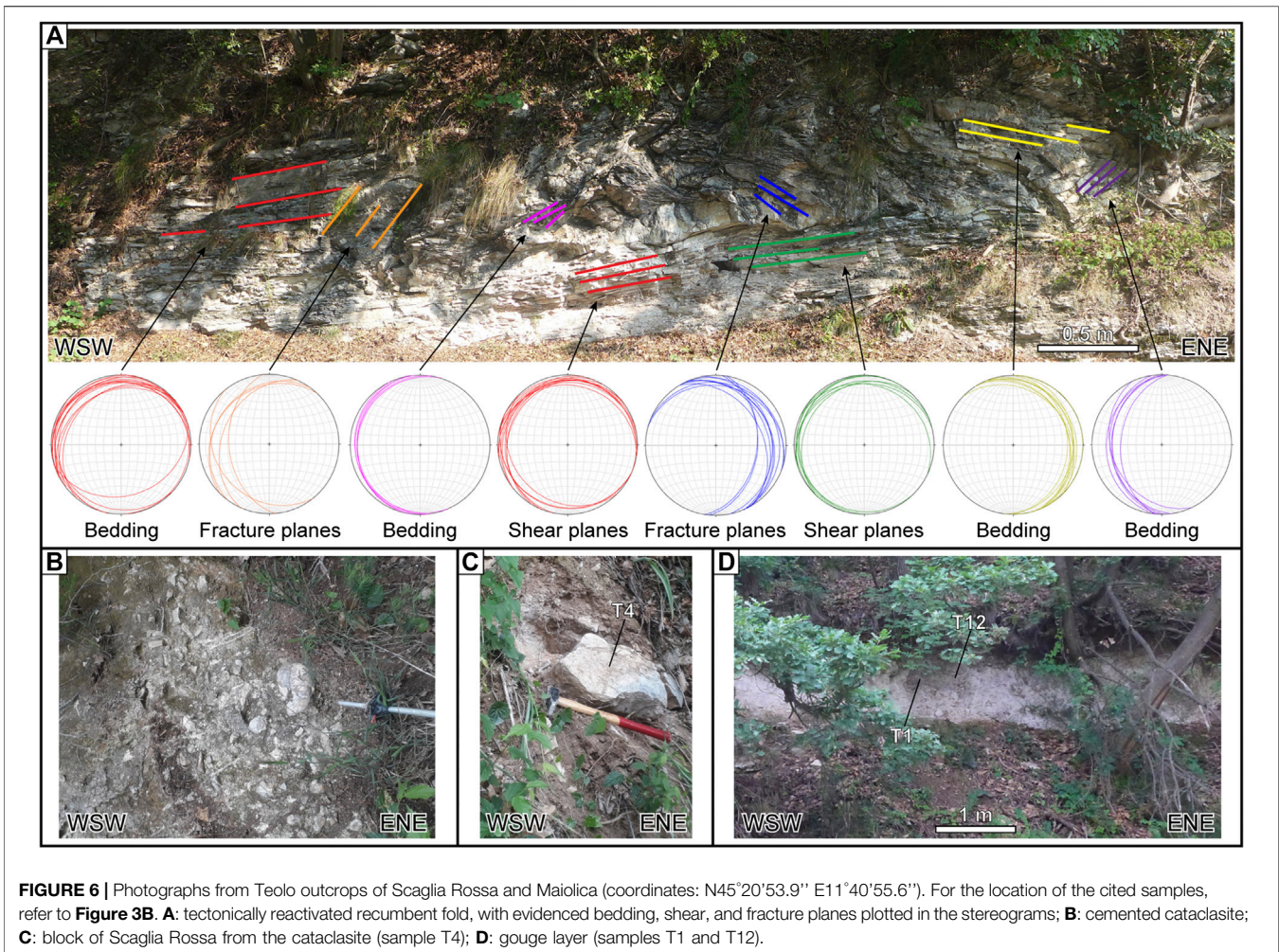
FIGURE 6 | Photographs from Teolo outcrops of Scaglia Rossa and Maiolica (coordinates: N45°20'53.9'' E11°40'55.6''). For the location of the cited samples, refer to **Figure 3B. A**: tectonically reactivated recumbent fold, with evidenced bedding, shear, and fracture planes plotted in the stereograms; **B**: cemented cataclasite; **C**: block of Scaglia Rossa from the cataclasite (sample T4); **D**: gouge layer (samples T1 and T12).

Rocca Pendice is one of the biggest dykes of the Euganean Hills (2.5 km × 200 m × 320 m of elevation). It is oriented NNW-SSE parallelly to the Schio-Vicenza Fault and ends at SSE against a fault of the NE-SW–oriented Riviera del Brenta system (Cucato et al., 2011).

To the west of the gouge layer, Scaglia Rossa is folded, as the underlying Maiolica, resulting in decametric complicated structures with red and black chert lenses and bands all deformed together (**Figure 6A**). The recumbent fold stays at the hanging wall of a thrust fault plane with a dip of 25° to the west, and the lower limb is pervasively foliated and elided by shear deformation. Hinges with two different geometries are recognizable: the first is rounded and typically found in synsedimentary folding, and the second is pointed. The rounded hinges are similar to the hinges of other folds observed in the Scaglia Rossa cropping out in this area either along the Euganean road bound to Teolo or in the Mt. Bignago quarry. These structures are interpreted as synsedimentary features or slumping. Maiolica cropping out in this area represents the upper part which typically ends with the Bonarelli event (Massari and Medizza, 1973; Gomez et al., 2002). Ten meters to the east of the fold, a ~5- to 6-m-thick cemented breccia is present and consists of massive blocks of

different lithologies (sample T4, Scaglia Rossa 1; **Figures 6B,C**). This breccia is covered by a cataclasite and a gouge layer about 1 m thick and 30 m long (samples T1 and T12; **Figure 6D**). This articulated package of rocks, breccia, and gouge is close to the thrust fault plane. Maiolica samples T13 (T13A and T13 B) and T14 are characterized by a black film over the surface and gray elements inside the rock. The gouge layer is covered by 0.3 m of Scaglia Rossa, largely disjointed by tree roots.

Geomechanical and Geotechnical Tests
Strength Tests

The behavior of the rocks and the processes which shattered and pulverized the Maiolica and Scaglia Rossa limestones have been investigated by means of uniaxial and triaxial compression and indirect tensile strength tests performed on cylindrical specimens with a length of 94.4–123.8 mm and diameter of 54 mm. These specimens were cored from anisotropic blocks of 20–80 cm in width and length. The height/diameter ratio for uniaxial and triaxial compressive tests ranges from 2 to 2.5 (ASTM D4543, 2005) or 2.5 to 3 times, following the International Society of Rock Mechanics standard methods (ISRM, 1978; ISRM, 1979; ISRM, 1983; ISRM, 2006). Many of the samples crumbled under coring or broke in disc-shaped samples so that the tests refer

exclusively to the rock having stronger mechanical characteristics. The best specimens of each lithology were used for triaxial and uniaxial tests, while the disc-shaped samples were processed for indirect tensile strength tests (Brazil test). Laboratory coring operation over blocks and little boulders are reported in **Supplementary Material 5, 6**.

The compression tests were performed in stress control mode with a testing machine (Controls MCC 8 mod. 45-C8622 scale 0–2000 kN, resolution 0.2 kN) that includes a suitable compression frame and a servo-hydraulic control console for applying an axial load to the specimen.

In the triaxial compression test, confining pressure was applied to the specimen by the Hoek cell with additional servo-hydraulic control. The specimen was placed in a rubber sealing membrane, and through it, the fluid cell exerted the confining pressure σ_3. In this study, pressures of 3, 5, and 8 MPa were applied. The confining pressure σ_3 and the axial stress σ_1 were increased simultaneously until the pre-established level of the confining pressure σ_3 was reached, and then the axial stress was increased at a constant rate until the failure occurred after 300 s of loading (usually 100–200 kPa/s were applied).

During the tests, all measurements (elapsed time, axial load, cell pressure, and vertical and horizontal strains) were recorded with the following frequency: one record every 0.5 s or 0.5 kN of increase in force applied. Both in the uniaxial and the triaxial tests, strain gauges were used for determining the vertical (axial) and the diametric (horizontal) strain of the specimen. The plots of stress–strain curves allowed determining Young's modulus and the Poisson ratio. However, in some cases, the horizontal strain measurements were not suitable due to the failure of the horizontal strain gauge, preventing the determination of the

Poisson ratio. The tensile strength test (Brazil test) was carried out on standard NX wireline cylindrical core of about 54 mm. A disc-shaped rock sample with a thickness approximately equal to the radius was placed between two compressing steel jaws with a radius equal to 1.5, the radius of the rock specimen. The load was applied continuously to the specimen at a constant rate until the failure occurs. Particular attention has been taken to detect the load of primary failure. The tensile strength of the specimen, σ_t, was calculated by the following formula:

$$\sigma_t = \frac{2P}{\pi D t} \quad (MPa),$$

where p is the load at failure (N), D is the diameter of the specimen (mm), and t is the thickness of the specimen measured at the center (mm). According to the ISRM, the recommended number of specimens per sample is ten. In this work, we measured five specimens of Maiolica and six of Scaglia Rossa to obtain a significative average value.

Failure Criteria

A rough evaluation of the test results is done with the Mohr–Coulomb failure criterion (Labuz, et al., 2012). According to this criterion, the peak strength can be mathematically approximated by linear expressions in a limited range of σ_3 according to $\sigma_1 = m\sigma_3 + \sigma_c$

The failure envelope for brittle material such as a rock is not linear (McClintock and Walsh, 1962; Hoek 1964; Cook 1965); thus, a linear envelope in the Mohr–Coulomb failure criterion is not suitable for rocks. Improving the research on the nonlinear failure criterion, Hoek and Brown (1980) proposed an empirical
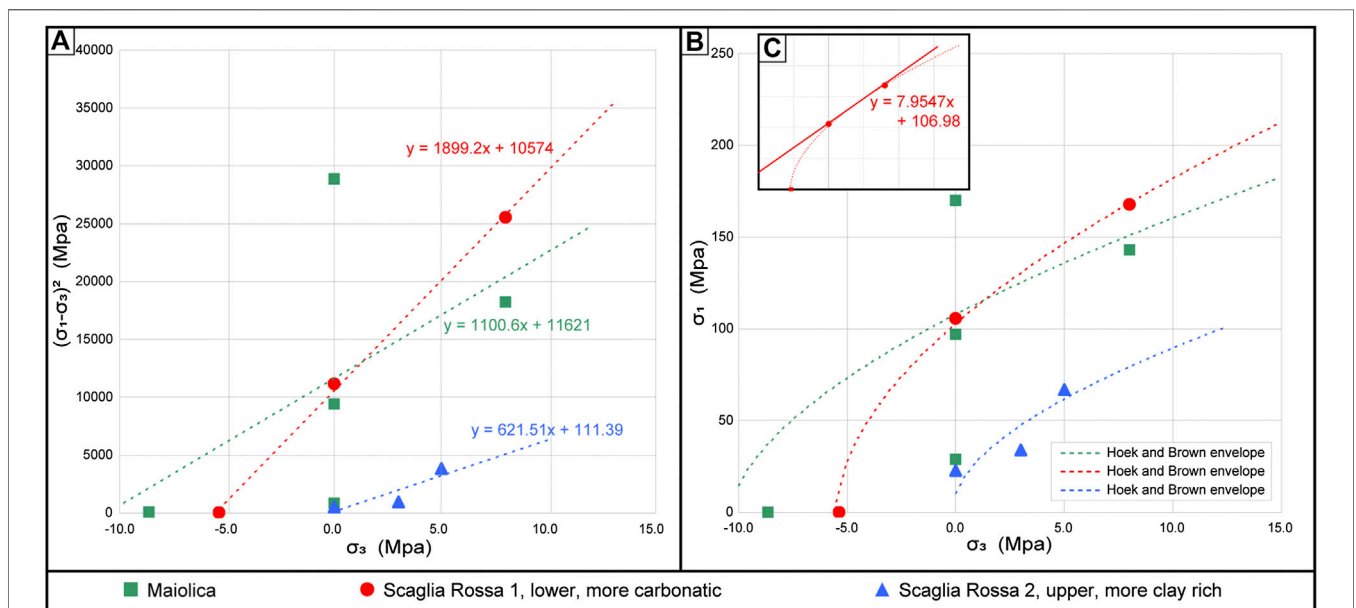

FIGURE 7 | Failure criteria. **A** $(\sigma_1\text{-}\sigma_3)^2$ vs. σ_3. Linear regression of the Hoek and Brown equation of Scaglia Rossa 1, Scaglia Rossa 2, and Maiolica. **B**: σ_1 vs. σ_3 envelopes. Mohr–Coulomb parameters from Hoek and Brown failure criterion. **C**: Mohr–Coulomb parameters of Scaglia Rossa 1 at the assumed value $\sigma_3 = 4.0$ MPa. The slope and the intercept of the tangent straight line give a friction angle $\phi = 51°$ and cohesion $c = 19.0$ MPa. Axes are the same as **B**.

equation to fit the results of a wide range of triaxial tests on intact rock samples (Hoek and Brown, 2018):

$$\sigma_1 = \sigma_3 + \sigma_{ci}\sqrt{m_i \frac{\sigma_3}{\sigma_{ci}} + 1},$$

where σ_1 and σ_3 are the major and minor principal stresses, respectively; σ_{ci} is the unconfined compressive strength, and m_i is a material constant for the intact rock. Then, the triaxial test results can be analyzed by linear regression of the Hoek and Brown equation (**Figure 7**)

$$(\sigma_1 - \sigma_3)^2 = \sigma_{ci} m_i \sigma_3 + \sigma_{ci}{}^2$$

The Hoek and Brown's failure criterion allows determining the Mohr–Coulomb parameters for the assumed value of the confining pressure σ_3 at which the Mohr–Coulomb parameters must refer. The position of the tangent line is fixed by the abscissa σ_3, the slope m, and the intercept σ_c of the tangent can be used for determining the internal friction angle ϕ and the value of apparent cohesion c in the sense of Coulomb's failure theory:

$$sin\varphi = \frac{m-1}{m+1}$$
$$c = \sigma_c \frac{1 - sin\varphi}{2cos\varphi}$$

Figure 7 shows the envelopes of Scaglia Rossa 1 (more carbonatic type), Scaglia Rossa 2 (clay enriched type), and Maiolica. The Mohr–Coulomb parameters for Scaglia Rossa 1 at the assumed value $\sigma_3 = 4.0$ MPa are represented; the slope and the intercept of the tangent straight line at $\sigma_3 = 4.0$ MPa give a friction angle $\phi = 51°$ and cohesion $c = 19.0$ MPa.

A number of samples were collected from each site but most of them crumbled during the coring or trimming operations. For this reason, the envelopes, at least in these cases, are constructed based on different samples from the same site (see samples VP23, VP24, VP25, and VP26 used for the indirect tensile strength (Brazil) tests, and specimens T4A and T4B from sample T4 used for the Brazil test). All the results obtained from geomechanical tests are reported in **Table 2**. Specimens ascribable to Maiolica generally show high values of Em (Young's modulus) spanning from 30 to 48 GPa. The value measured on the sample AP20 (Scaglia Rossa) from Mt. Bignago is also high (36.7 GPa), while sample T4 (A and B) from Teolo shows an anomalous value of 55.6 GPa. The mechanical properties of Maiolica and Scaglia Rossa 1 are comparable and differ significantly from those of Scaglia Rossa 2 (see **Figure 7**). For comparison, the mechanical parameters of three magmatic rocks (samples VP6, VP15, and AP17) are reported in **Table 1** and in the **Supplementary Material 5**. They show Em values ranging from 8.3 to 26.1 GPa, thus much lower than those obtained from Scaglia Rossa 1 and Maiolica. The geomechanical tests performed in the laboratory resulted in the splitting of sample VP6 (rhyolite) and the shattering of samples VP15 (andesite) and AP17 (perlite) (**Supplementary Material 5**).

An estimation of the dissipated strain energy up to the peak stress was possible by calculating the area below the axial stress vs.

TABLE 2 | Results from uniaxial and triaxial compression and indirect tensile strength tests. Colors corresponds to those used in **Figures 7,8**. Symbols: d = specimen diameter; L = specimen length; γ = unit weight; ε_{AMAX} = maximum axial strain; E_{diss} = dissipated strain energy up to the peak stress; σ_3 = confining pressure applied in the triaxial tests or tensile strength value in the indirect tensile (brazil) tests; σ_1 = peak axial stress; Em = Young's modulus; ν = Poisson ratio. Damage: I = macroscopically intact; Sp = split; SH = shattered; F = incipient and prominent fragmentation; f = sample faulted.

| Lithology	Test	Sample	D	L	γ	Stress rate	Strain rate	ε_{AMAX}	E_{diss}	σ_3	σ_1	$(\sigma_1-\sigma_3)^2$	Em	ν	Damage
			mm	mm	kN/m³	kPa/s	mm/min	%	MJ/m³	MPa	MPa	MPa	GPa	—	
Maiolica	Uniaxial	VP10	53.01	108.9	24.765	100	—			0	28.7	823.69	48.0	0.14	I
Maiolica	Triaxial	T13 A- a	52.85	123.8	24.352	200	—	0.45	0.54	8.0	143.0	18,225	34.8	0.37	SH
Maiolica	Uniaxial	T13 A- B	52.96	98.0	24.164	200	—	0.47	0.23	0	97.0	9,409	21.7	0.17	F
Maiolica	Uniaxial	T14 A	54.54	94.4	24.875	100	—	0.57	0.51	0	169.9	28,866	30.8	0.22	SH
Maiolica	Brazil test	VP23-VP24-VP25-VP26 (average)	54.06	27.26	25.013	—	1.000	—	—	-8.64	0	74.6496	—	—	Sp
Scaglia Rossa 1	Uniaxial	AP20	52.95	94.2	23.593	100	—	—	—	0	105.6	11,151.4	36.7	0.28	SH
Scaglia Rossa 1	Triaxial	T4A	52.97	113.4	25.281	200	—	0.30	0.30	8.0	167.8	25,536	55.6	—	I
Scaglia Rossa 1	Brazil test	T4A-T4B-AP28-AP32 (average)	53.517	28.4	24.215	—	1.000	—	—	-5.37	0	28.8476	—	—	Sp
Scaglia Rossa 2	Uniaxial	AP29	53.51	105.71	22.338	100	—	—	—	0	22.8	519.84	23.8	—	F
Scaglia Rossa 2	Triaxial	VP18	52.94	105.4	24.508	100	—	0.24	0.04	3.0	33.9	954.81	8.4	—	Sp + f
Scaglia Rossa 2	Triaxial	AP30	53,52	117.1	22.789	100	—	0.36	0.16	5.0	66.9	3,831.61	15.3	0.13	I
Rhyolite	—	VP6	52.89	122.7	20.178	200	—	0.49	0.18	0	49.5	2,450.25	8.3	0.20	F
Andesite	—	VP15	53.22	101.2	23.350	200	—	—	—	0	38.5	1,482.25	26.1	0.33	F
Perlite	—	AP17	52.94	109.7	23.172	200	—	—	—	0	113.0	12,769	22.3	0.25	SH
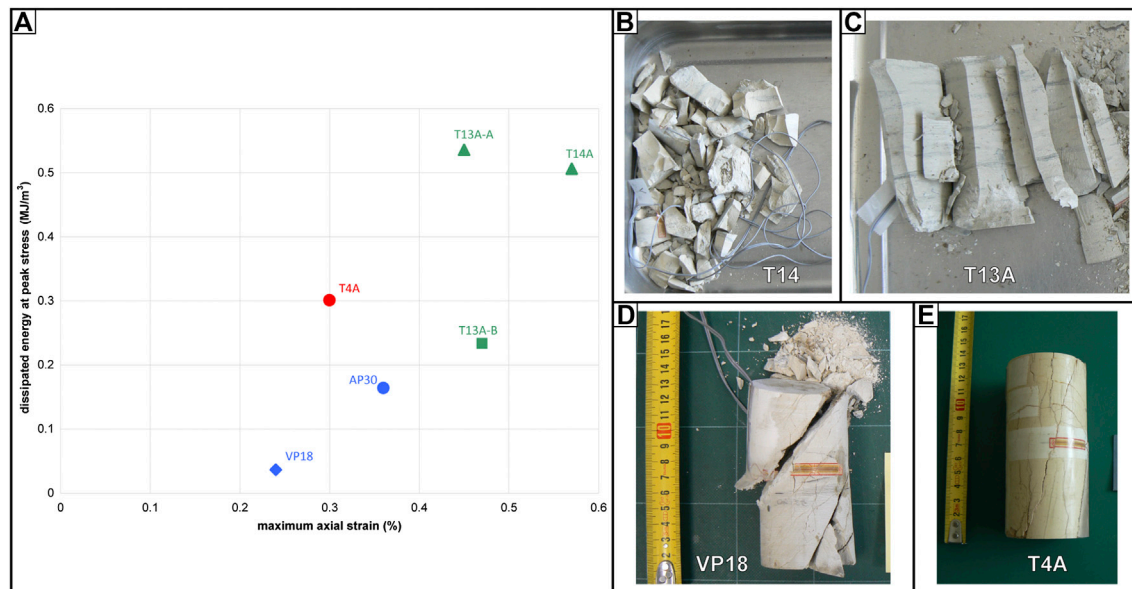
FIGURE 8 | Results of geomechanical tests. **A:** Plot of dissipated strain energy at the peak stress vs. maximum axial strain. **B:** Shattered specimen of Maiolica T14 A (uniaxial test); **C:** incipient and prominent fragmentation of specimen of Maiolica T13 A-B (uniaxial test); **D:** split and faulted specimen of Scaglia Rossa 2 VP18 (triaxial test); **E:** intact specimen of Scaglia Rossa 1 T4A (triaxial test).

axial strain curves and the damage produce by the energy dissipation (**Figure 8**). This estimation was possible only for specimens where the vertical strain gauge was not subject to damage up to the failure. Shattered samples are generally characterized by much higher axial strain and higher energy dissipated up to the peak stress (**Figure 8**). The dissipated strain energy is proportional to the damage of the specimens; shattered specimens were obtained when the strain energy exceeded the threshold of about 0.5 MJ/m^3 (**Figure 8**).

Gouges

Four samples were taken from the Scaglia Rossa gouges and cataclasites: AP1 and AP4 from Mt. Bignago, and T1 and T12 from Teolo (**Figures 2, 6**). In particular, 1) sample AP1 was collected from the cataclasite at the border of the quarry below the synsedimentary reactivated fold; 2) sample AP4 comes from the flour powder layer on the top of the Mt. Bignago quarry; 3) samples T1 and T12 were taken from the gouge layer along the road between the villages of Teolo and Villa di Teolo, to the east of the recumbent fold. Two further samples were collected from a gouge layer (VP9) and a pocket (VP14) within Maiolica, in Val Pomaro. From a geotechnical point of view, the material was considered comparable to soil, and it was therefore classified by performing, in most of the samples, the following geotechnical tests: 1) particle-size distribution (gradation) of soil using sieve analysis (ASTM D6913/ D6913M - 17, 2005), 2) particle-size distribution (gradation) of fine-grained soil using the sedimentation (hydrometer) analysis (ASTM D7928-17, 2005), and 3) liquid limit, plastic limit, and plasticity index of soil (ASTM D4318–17e1, 2005). Based on the Atterberg test, results carried out on 0.074 mm

passing grain size material and using the plasticity chart, samples can be classified as silt with low plasticity (ML in the USCS classification; **Figure 9A**; ASTM D2487–17, 2005). T1 sample is the only exception, being classifiable as silty sand (SM). Nonetheless, the particle size distribution of T1 slightly differs from that of AP1 and T12 (**Figure 9B**), all of them having a percentage of fine material ranging between 40 and 51. These three specimens, coming from Mt. Bignago (AP1) and Teolo (T1 and T12), likely indicate a similar origin (**Figure 9B**). Sample AP4, instead, has a higher percentage of fine material (96%), probably due to more intense crushing and pulverization of the material.

Finally, ring shear tests (ASTM D6467-13e1, 2005) were performed on specimens obtained from samples AP1, AP4, T1, and T12. This test was used to determine the torsional ring shear by means of the residual shear strength of cohesive soil under drained conditions. The test is performed by deforming a reconstituted specimen at a controlled displacement rate until the constant drained shear resistance is offered on a single shear plane, fixed by the configuration of the apparatus. The drained residual failure envelope was determined by applying three different normal stresses in the range of 15.3–61.9 kPa. The rupture occurred along a fixed shear plane extremely thin, and the residual value of shear strength was determined to give a large amount of continuous shear displacement. The residual shear strength is between 34° and 35°, which are unusual values for similarly classified materials in the geotechnical field. These high values probably depend on the presence, along the shear plane, of high-resistance small rough pieces of poorly crushed material, derived from microfragmentation of Scaglia Rossa.
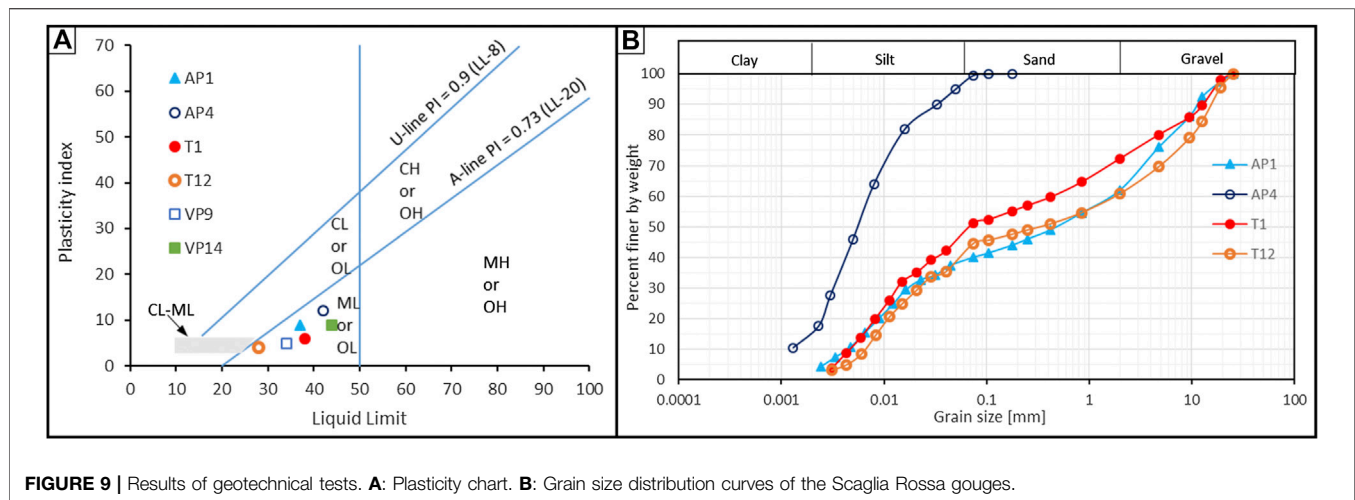
FIGURE 9 | Results of geotechnical tests. **A**: Plasticity chart. **B**: Grain size distribution curves of the Scaglia Rossa gouges.

Seismic Survey

Seismic velocities of the fragmented, shattered, and pulverized Scaglia Rossa were measured at Mt. Bignago, over and laterally with respect to the quarry, along the road to Arquà Petrarca. The trace of the seismic surveys and the diagrams obtained are reported in **Supplementary Material 7**. The compressional P-wave and shear S-wave velocities were determined along the same seismic acquisition, allowing the *in situ* estimation of the Poisson module to be compared with the geotechnical tests on specimens.

For the seismic characterization, we used a Geode digital seismograph with 24 geophones, in both vertical and horizontal orientation (P-wave survey: geophone vertical, 15 Hz, spacing 2 m over 46 m in length; S-wave survey: geophone horizontal, 15 Hz, spacing 1.5 m over 34.5 m in length) and a 5 kg seismic hummer as the source. Since the target of the survey was to characterize the shallower layers, the total length was limited, increasing the spacing resolution between receivers. For both P-waves (v_p) and S-waves (v_s), survey refraction tomography based on first break methods was adopted. The source for P-wave was a vertical impacting hammer with electric trigger, while for the S-wave, we adopted a horizontal hammer/beam system, energized at both sides to help S-wave phase reconstruction.

The first arrivals were then inverted for P- and S-wave velocity distribution using a refraction tomography approach with Seisimager/2D software. The dynamic Poisson module (ν) was obtained from P- and S- wave velocities, with the formula (Lacy, 1997):

$$\nu = \frac{v_p^2 - 2v_s^2}{2\left(v_p^2 - v_s^2\right)},$$

where v_p is the P-wave velocity and v_s is the S-wave velocity of the surveyed layer.

Results of the seismic survey highlight that cataclastic material of the Mt. Bignago observed within the upper wall of the Contarine quarry (**Figure 4**) lies between an upper unconsolidated layer, with low v_p and v_s velocities ($v_p = 450$–500 m/s, $v_s = 280$–330 m/s), and a deeper consolidated

rock layer at a depth greater than 5–7 m with $v_p = 2000$ m/s and $v_s = 1,100$ m/s.

In between, at a depth of 2–3 m, the cataclastic material layer object of this study presents an S-wave velocity of 600 m/s and a P-wave velocity of 1,100 m/s. The dynamic *in situ* Poisson ratio of the cataclastic material is 0.29, in agreement with the results of the geotechnical tests (**Supplementary Material 7**). The seismic acquisition so confirmed the presence of this semi-consolidated layer with poor mechanical quality and a thickness of 2–3 m.

Global Navigation Satellite System Analysis

To understand the dynamic processes presently active in the Euganean Hills, and whether they can be compared with the past processes responsible for the formation of gouges and/or for their exposure at the surface, we investigated the present geodynamic scenario of the Venetian region. We have estimated the horizontal and vertical kinematic patterns using the GNSS (global navigation satellite system) daily observations acquired in the January 1, 2001–December 31, 2019 time span. Data acquired with a 30-s sampling rate have been analyzed using the procedure described in **Supplementary Material 8**.

The horizontal Eurasia-fixed velocity field and deformation pattern are shown in **Figures 10A,B**. The most striking features of the deformation pattern are observed in the eastern sector of the Italian peninsula. A shortening regime with NNW-SSE pattern in the Eastern Alps, at the northern collisional border between the Adriatic Plate and the Eurasian domain, is visible. A roughly N-S compression occurs in the central area of the Po Plain eastern sector, overlying the outer buried Northern Apennine. The shortening axes (red arrows in **Figure 10B**) spin roughly in NE-SW direction in the easternmost area of the Po Plain, while a transcurrent regime (white area) mainly occurs in correspondence of the Schio-Vicenza Fault area. The strain rate values estimated in this area are ~10–30 nanostrain per year as also estimated by other authors (Cenni et al., 2012; Riguzzi et al., 2013; Serpelloni et al., 2016). The present kinematic and deformation patterns suggest a sinistral movement of the Schio-Vicenza Fault, obtained with a distance decay factor of 50 km; the present distribution of GNSS permanent stations does not allow
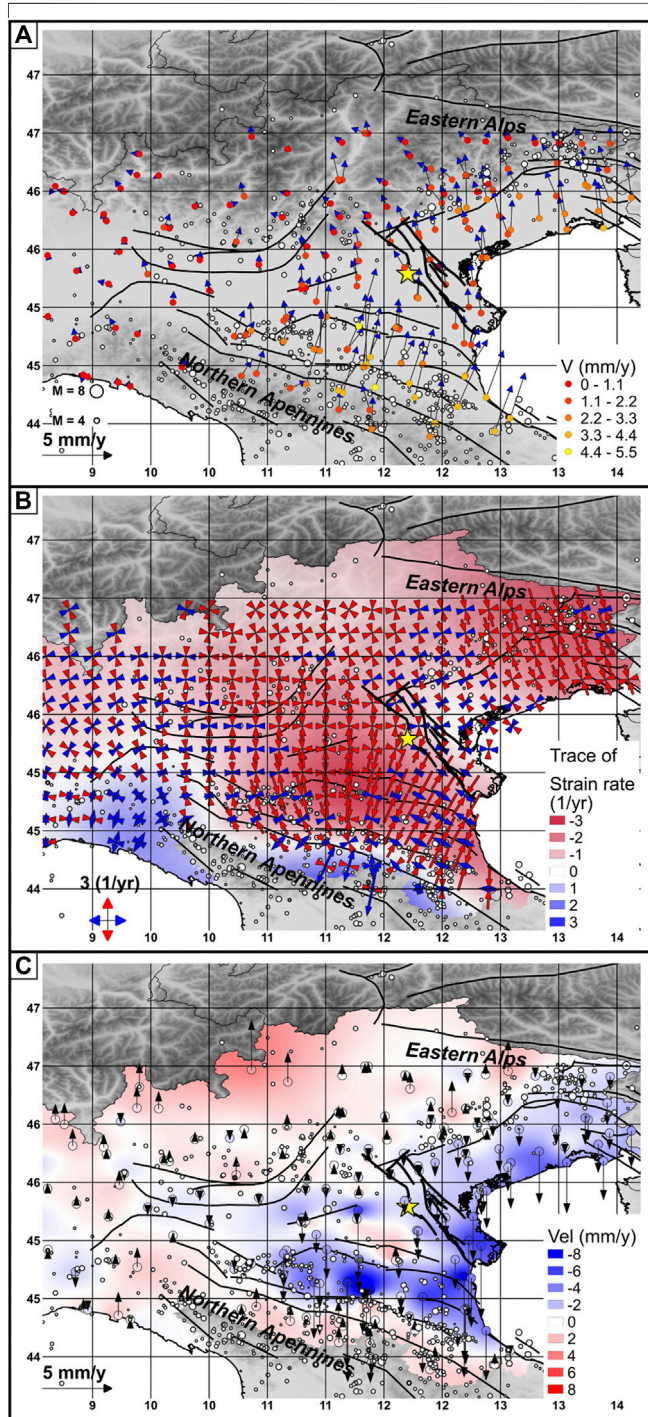
FIGURE 10 | GNSS kinematic and deformation patterns in the study area and surroundings. **A**: Present horizontal pattern in the NE Italy with respect to fixed Eurasia, modeled using the Euler pole (Altamimi et al., 2016). Color of the circles indicating the position of the GNSS permanent stations is proportional to the modulus of the horizontal vector following the scale given on the left corner of the figure. White circles: seismic events (Rovida et al., 2020); black lines: the trace of the normal, reverse, and strike-slip faults from the Euro-Mediterranean database
(Continued)

for investigation of tectonic processes with a wavelength lower than 50 km. The observed displacements are consistent with the inferred geodynamic role of the Schio-Vicenza Fault, that is, to accommodate to the east the indentation of Adria against the Southern Alps (e.g., Mantovani et al., 2020 and reference therein).

Figure 10C shows the present vertical kinematic pattern: the uplift in the alpine area and the lowering of the eastern sector of the Po and the Venetian plains are clearly observable. The GNSS results indicate that the Schio-Vicenza Fault area is interested by subsidence of ~1 mm/y, with an enhanced lowering in the southern sector. The vertical displacements are the result of both natural and anthropogenic sources. Several studies proposed that anthropogenic factors prevail over tectonic processes in causing the subsidence of the Venetian Plain (e.g., Cenni et al 2013; Corbau et al 2019).

RESULTS AND DISCUSSION

Shattered Rocks, Cataclasites, and Gouges

In the study areas, rocks ascribable to Maiolica and Scaglia Rossa were found fragmented, shattered, and pulverized in three sites of the Euganean Hills. The gouges are classified as "pulverized rocks" because the fragmentation process produces centimeter-scale fractures (Dor et al., 2006). Even though the Euganean Hills are a thermal area (e.g., at Abano Terme and Montegrotto Terme), no alteration due to thermal water circulation has been detected in the three sampled sites.

At Mt. Bignago, the gouge layer of the main outcrop (site 7 and Via Bignago, site a, in **Supplementary Material 1**) does not show shear diagnostic microstructures (i.e., mirror-like slip surfaces or truncated clasts in the gouge) and this setting is "quasi-static" (photograph E in **Figure 4**). This evidence seems to exclude a significant shear deformation when the gouge AP4 formed under tensile load. In other sites where pulverized carbonate or intensely fractured rocks have been observed, such as in southern Italy (i.e., Mattinata Fault), pulverization has been interpreted as evidence of seismic fault slip (Billi and Storti, 2004). In the case of Mt. Bignago, if a slipping zone is present, it is covered by cataclasites. The absence of shear diagnostic microstructures in the visible portion of the outcrop does not exclude a dynamic

FIGURE 10 | of seismogenic sources (SHARE project, Basili et al., 2013). Bold black lines: the Schio-Vicenza Fault planes (Pola et al., 2014). Yellow star: location of the Euganean Hills. **B**: Horizontal strain rate field in 10^{-8} 1/y estimated using the grid strain rate approach (Teza et al., 2008; Pesci et al., 2010; Cenni et al., 2012). Red converging and blue diverging arrows indicate principal axes of shortening and lengthening, respectively. The strain rate field has been estimated using a decay factor of 50 km and a grid spacing of about 20 km. Color contour represents the trace of the strain rate matrix values following the scale given in the upper left corner. Blue and red areas indicate, respectively, where lengthening and shortening are the dominant deformation patterns. The strike-slip areas are highlighted in white color. Legend as in **A**. **C**: Vertical kinematic pattern in NE Italy. Color of the circles that indicate the position of the GNSS permanent stations is proportional to the modulus of the vertical values following the scale reported on the upper left corner of the figure. Legend as in **A** and **B**.

TABLE 3 | Recent earthquakes (database from INGV and OGS - http://terremoti.ingv.it, http://www.crs.inogs.it) occurred in the province of Padova since 1977 and the relevant historical earthquakes that significantly damaged the city of Padova (e.g., the collapse of the Carmelite Church, Guidoboni et al., 2007).

Recorded earthquakes

Local date	Locality	Latitude	Longitude	Magnitude Ml	Depth (km)
July 10, 1977, 17:56	Lozzo Atestino	45.2860	11.6450	2.4	20.1
September 03, 1984, 9:33	Mestrino	45.4350	11.8130	2.1	19.2
November 11, 1987, 00:49	Lozzo Atestino	45.3330	11.6680	2.4	2.5
March 28, 1988, 17:26	Este	45.1700	11.6100	2.3	19.7
August 16, 1996, 05:58	San Pietro	45.2370	11.8330	2.4	5
June 1, 1998, 14:38	Piacenza d'Adige	45.2000	11.9230	2.8	24
September 15, 2001, 18:01	Galzignano Terme	45.3940	11.7190	2.8	5
March 03, 2003, 06:04	Montegaldella	45.2270	11.6760	2.8	5
July 11, 2005, 07:05	Teolo	45.3630	11.6760	3.1	7
January 05, 2013, 21:26	Sant'Urbano	45.1360	11.6270	3.3	6
October 30, 2015, 19:45	Tribano	45.2152	11.7960	2.0	10
November 09, 2019, 22:46	Granze	45.1500	11.7200	2.0	7

Historical earthquakes

1004 (?)	Padova	—	—	?	—
1485 (?)	Padova	—	—	4.5	—
01–1491	Padova	—	—	5	—

shear rupture. The E-W trending fold deforming the Mt. Bignago gouge, the underlying cataclasite, and the overlying Scaglia Rossa look like as a fault-related fold, but the shear plane is not visible (photograph C in **Figure 4**). Similarly, the recumbent fold in Maiolica and Scaglia Rossa ramping up near breccia and cataclasite along a west-dipping thrust fault plane near Teolo seems to confirm a dynamic shear rupture associated with a transpressive activation of pre-existing fault planes (photograph A in **Figure 6**).

Pulverization

Pulverization of Scaglia Rossa 1 and Maiolica produced gouges having similar features (**Figure 9B**), but the Mt. Bignago gouge is found to be finer (LM in **Figure 9B**, grain size of <100 μm) than those of Val Pomaro and Teolo (grain size greater than 100 μm), suggesting either enhanced damage or a greater strain rate. Pulverization to fine grain size, like that present at Mt. Bignago, requires high energy and/or high strain rate. If the rock had been predamaged, it would be easier to pulverize it. Successive loadings might be able to produce similar results if compared with those obtained from a single shear event (Doan and d'Hour, 2012). Pulverization was not observed in the subvolcanic rocks (i.e., rhyolite, andesite, and perlite) and in Scaglia Rossa 2. These lithologies are both characterized by a relatively low Em value, in the range 8–26 GPa, that might explain the absence of pulverization.

In the Southern Alps, pulverization has been recently described along a strike-slip branch of the Schio-Vicenza Fault at Borcola Pass and along the Foiana strike-slip fault in dolostones (Fondriest et al., 2012; Fondriest et al., 2015; Fondriest et al., 2017). The Schio-Vicenza Fault branch is characterized by a >80-m-wide damaged zone which has been exhumed from a depth of ~1.6–1.7 km. The Foiana Fault is ~30 km long, characterized by a <300 m damaged zone exhumed from a depth >2 km. These types of

pulverized rocks seem to form only at shallow depths (<3 km, Billi et al., 2003; Fondriest et al., 2017). In the Euganean Hills, the depth at which pulverization occurred could have been in the range 1–5 km. Here, a thickness of ~1 km for the Eocene and Oligocene sequences is reported (Proto Decima and Sedea, 1970; Piccoli et al., 1976), and this suggests that the pulverization occurred at a minimum depth of 1 km. If the slip rate of the frontal part of the Euganean Hills was at least 0.4 mm/y, as estimated by Livio et al. (2020) for Mt. Netto near Brescia, and by Anderlini et al. (2020) for the Montello thrust, then ~2$10^6$ years could have been sufficient to deform and expose the Scaglia Rossa after the formation of the gouge layer.

Rocks can be pulverized under a tensional load such as that generated by an earthquake occurring within the tip of a fast propagating fault (Rice et al., 2005; Wilson et al., 2005). Pulverization usually occurs along strike-slip faults characterized by large earthquakes with M >7, such as the San Andreas, North Anatolian, and Arima-Takatsuki faults (Brune, 2001; Mitchell et al., 2011). According to Wilson et al. (2005), the parameters which govern the formation of the gouge can be related to the "earthquake processes" and not necessarily cumulative slip attrition. Therefore, a unique earthquake can pulverize the rocks by a sequence of fault-normal unloading and loading when the rocks are still deeper, during the earthquake passage, or at the tip of an earthquake rupture (Reches et al., 2005; Rice et al., 2005).

In the cases of Mt. Bignago or Teolo, the gouge layers are not far from the Schio-Vicenza Fault which has been active as a normal fault since the Cretaceous and has been reactivated as a strike-slip during the Neogene (Massironi and Zampieri, 2007). Its activity could have predamaged the rocks predisposing them to a successive pulverization (see discussion about pulverization along the SEMP fault, Schrockenfuchs et al., 2015; Fondriest et al., 2017). In the studied rocks, pulverization did not obliterate the
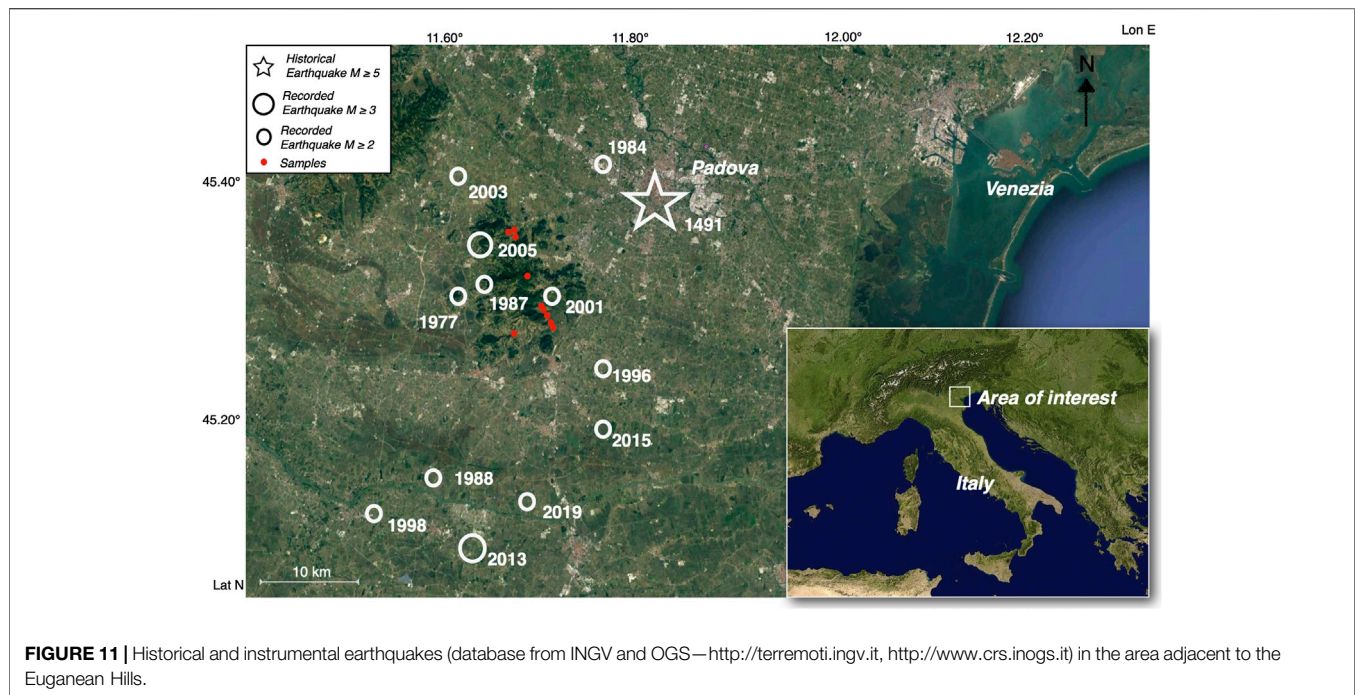
FIGURE 11 | Historical and instrumental earthquakes (database from INGV and OGS—http://terremoti.ingv.it, http://www.crs.inogs.it) in the area adjacent to the Euganean Hills.

mesoscopic sedimentary structures; thus, a unique event, rather than multiple, seems to have been responsible for the pulverization when Scaglia Rossa and Maiolica were confined below Eocene and Oligocene sequences.

Role of the Schio-Vicenza Fault and of the Prealps and Apennine Tectonics

The cataclasite and gouge development at depth and the successive deformations, as the folding observed at Mt. Bignago and the recumbent fold ramping up over the cataclasite at Teolo, can be attributed to the compression related to the sinistral strike-slip Schio-Vicenza Fault. This setting is similar to that of the S- to SE-vergent thrusts of the Venetian Prealps (Burrato et al., 2008; Fantoni and Franciosi, 2010; Vannoli et al., 2015). However, the final exhumation and exposure of Maiolica and Scaglia Rossa gouges and cataclasites at the bottom of the Teolo valley (50 m a.s.l.) and at Mt. Bignago (50–80 m a.s.l.) could also be attributed to the Northern Apennines thrust tectonics (Livani et al., 2018 and reference therein). These thrusts are still seismically active at shallow depth below the Po Plain as indicated by the Emilia earthquakes occurred in 2012 (Vannoli et al., 2015). The Po Plain sector lying to the west of the Schio-Vicenza Fault is indicated as an area where the Southern Alps and Apennine thrusts cannibalize the Adria foreland (Serpelloni et al., 2016; Brancolini et al., 2019). Since the early Pleistocene, the northern Adriatic region has been affected by significant subsidence (Ghielmi et al., 2013). This process has been linked to the NE-ward migration of the Apennine foredeep or, in the alternative, to the lithospheric flexure controlled by the northward motion of the Adria (Carminati et al., 2003).

The S- to SE-vergent thrusts westward of the Euganean Hills and the Hills themselves are interpreted as the consequence of the Adria Moho uplift, from 40, below Lake Garda, to 28 km, below the Euganean Hills, in depth (see Figure 3F in Scarascia and Cassinis, 1997). The shallow Moho depth is indicated by the deep-rooted positive gravity anomaly measured in correspondence of the Milano frontal thrust belt, the Berici, and Euganean hills (Morelli, 1951; Norinelli, 1963; Scarascia and Cassinis, 1997; Zanolla et al., 2006). In the Euganean and Berici hills area, relatively high-density rocks have been identified by tomography (Viganò et al., 2013).

Damage of Specimens and Dissipation of Energy

Maiolica and Scaglia Rossa 1 show comparable mechanical properties and are significantly different from Scaglia Rossa 2 (**Figures 7,8**). Maiolica shows greater variations both in the damage rate and in the peak axial strength (cf. specimens VP10 and T14). The presence of a micro-fragmentation in VP10, collected from an outcrop deformed by both NNW-dipping shear planes and SW-dipping fault planes (stereoplot C in **Figure 3**), decreases the mechanical properties of the sample.

The dissipated strain energy is proportional to the damage of the specimens. For our samples, energy was obtained when the strain energy exceeded the threshold of about 0.3–0.5 MJ/m^3 (**Figure 8**) (**Table 2**). These measures demonstrate that higher strain energy (or more elevated strain rate) should be necessary to pulverize the rocks more than shattering them. According to Wilson et al. (2005), the energy consumed in "quasi-static" laboratory experiments is 0.2–0.3% of the supplied mechanical energy, while the energy consumed by friction to produce gouge

during an earthquake is about 50% of the total earthquake energy (Scholz, 2002). This means that the pulverization observed in the field required much higher energy than that consumed in the laboratory experiments to produce shattering.

Seismogenic Sources

The studied sites of the central Venetian Plain have not been recently interested by relevant seismic activity (Poli et al., 2008). Nevertheless, in the past, few important earthquakes were located in the southern district of Padova (Guidoboni et al., 2007; **Table 3**). In particular, the earthquake occurred in 1491, with an estimated magnitude (M) equal to 5, generated severe damage in the city monuments. The damage observed in Maiolica and Scaglia Rossa (max: 0.5 MJ/m^3) suggest the formation of the gouge to be related to one or more events with a magnitude bigger than the modern earthquakes (M <3.5).

On the other hand, several local weak seismic activities were recorded in the studied area during the last 40 years, since a seismographs network was installed (Priolo et al., 2007; **Table 3**). In particular in the Euganean Hills area, several small earthquakes occurred with hypocenter generally located in the first 6 km (**Table 3**). The local seismic events are concentrated in the western sector of Padova Province, revealing an ongoing activity in the Euganean Hills. This diffused seismic activity is probably linked to the Schio-Vicenza Fault that divides the eastern and western sectors of the low Venetian plain (Pola et al., 2014).

The area is characterized by a low-level distributed seismicity that is not enough to produce the pulverization of the rocks observed at the outcrops. The paleo-earthquake magnitudes in the studied area suggest moderate events that, considering classical energy distribution (Wells and Coppersmith, 1994), can hardly generate gouge. If these rocks were seismogenic in origin, they should be related to shallow moderate seismic events linked to the Schio-Vicenza Fault, with released energy comparable with the historical earthquake located in the area in the XV century (M = 5). In this case, we must take into consideration that comparable low energy may have led to rock pulverization in the carbonates, as supported by the results of the laboratory rupture analysis. An alternative hypothesis, as proposed for dolomite (Schrockenfuchs et al., 2015), is that the pulverization is not the evidence of a seismogenic source, but rather comes from induced slip on rough faults with heterogeneous stress conditions in the nearby of the main plane.

Deformation Pattern and Geomorphological Evolution of the Euganean Hills

Due to different degrees of erodibility of the sedimentary cover, the laccolites and dykes of the Euganean Hills were slowly exhumed at the end of Miocene, and a complex landscape made of gentle slopes and rounded peaks was shaped (Mozzi, 2001; Mozzi et al., 2013). On the contrary, the rare presence of acid volcanic rocks, more resistant to erosion, gave birth to subvertical rocky walls as for instance that of Rocca Pendice (Cucato et al., 2012). The Euganean Hills are connected to the alluvial plain by a widespread skirt of colluvium, mainly

developed during the glacial phases due to frost weathering (ARPAV, 2005). The formation of the alluvial plain was influenced by megafan formation of the Brenta River, to the north and the east, and of the Adige River, to the south (Fontana et al., 2014). The alluvial plain mainly formed during the Last Glacial Maximum (LGM), when the Brenta River deposited up to 30–35 m of sediments (Cucato et al., 2012; Rossato et al., 2018) with a sedimentation rate ranging between 1.8 and 3 m/ky (Rossato and Mozzi, 2016). At the glacial decay (i.e., about 18 ka ago), these sediments were deeply and rapidly entrenched by the rivers that excavated several incised valleys up to 45 m below the surface of the plain (Fontana et al., 2014). At the apical portions of the megafans, the rivers flowed into such incised valleys since then, but in the lower tracts (near the Euganean Hills), the incisions were mostly filled, and aggradation took place once again over the LGM plain.

The estimated vertical slip rate of the Euganean Hills is at least 0.4 mm/y once compared with Mt. Netto (Livio et al., 2020) and Montello (Anderlini et al., 2020). Even though during glacial stages, the alluvial plain grew remarkably faster than the Euganean Hills (3–7.5 times faster during the LGM), the uplift of the latter could have filled the gap during interglacial times, when the alluvial sedimentation was lower.

During the Holocene, the Brenta River flowed some kilometers eastward of the study area, while the Adige River flowed just south of the Euganean Hills during the Bronze Age and the Roman times (Piovan et al., 2010). During the late stages of the LGM and the Holocene, there is no evidence that either the Adige or the Brenta rivers crossed the corridor between the Berici and the Euganean hills (ARPAV, 2005), in correspondence of the main Riviera del Brenta Fault. The uplift of the Euganean Hills most probably played a fundamental role in creating an effective watershed between the northern and the southern sedimentary domains.

CONCLUSION

A tectonic compressive deformation similar to that of the Venetian-Friulian thrust belt, and possibly of the same age (Pleistocene), is present in the Euganean Hills. This compressive tectonic setting is displaced southward by the sinistral activity of the Schio-Vicenza Fault. The Euganean Hills are positioned in front of the Apennine frontal thrusts, and their uplift is likely related to such tectonic regime.

The present kinematic and deformation patterns, estimated by the GNSS permanent sites, confirm the sinistral movement of the Schio-Vicenza Fault. This fault is characterized by a strain rate of a few tens of nanostrain (10–30 1/y), a result that is in agreement with the seismicity of this area. The present distribution of the GNSS sites (mean inter-distance of ~50 km) does not allow for estimation of a more refined deformation pattern in the Schio-Vicenza Fault area. Alluvial sedimentation continuously covers the foot slopes of the Hills, hindering their deformation and uplift. Moreover, the Venetian Plain eastward of the Euganean Hills is influenced by a subsidence of ~1 mm/y, due to both natural and anthropogenic processes.

In three sites in the Euganean Hills, shattered material, cataclasites, and gouges, similar to the pulverized rocks classically described from major faults with larger earthquakes (up to M >7), are found within Maiolica and Scaglia Rossa. Micropaleontological analyses indicate that the gouges derive from the fragmentation of the adjacent pristine carbonatic rocks. Outcrop observations show a "quasi-static" setting of the gouges. Geotechnical analyses confirm a silty sand to silty composition of the gouges and their anomalous high residual shear strength (34–35°). Structural analyses carried out in two localities located to the south (Mt. Bignago) and to the northeast (Teolo) of the Euganean Hills suggest that cataclasites and gouges are likely related to compression that occurred at shallow depths (1–2 km). A dynamic shear rupture is suggested by the recumbent fold in Maiolica and Scaglia Rossa ramping up over the cataclasite, along a west-dipping thrust fault plane near Teolo. At Mt. Bignago, no shear diagnostic microstructures or visible shear plane have been observed, but this cannot exclude the presence of this structure in the underground.

Geomechanical analyses on rocks near to gouges confirm the high strength of the Maiolica and carbonatic Scaglia Rossa 1 (Em: 30–48 GPa) in respect to clay-rich Scaglia Rossa 2 (Em: 8–24 GPa) and to subvolcanic rocks (Em: 8–26 GPa). Carbonatic rocks loaded to the failure through static uniaxial compression, split, and shattered; at failure, high energy was dissipated (0.3–0.5 MJ/m^3). No pulverization occurred during these tests. If the pulverization observed in the field was caused by seismic deformation, the triggering earthquake(s) was (were) bigger than those recorded in the Euganean Hills area (M ≤5). Alternatively, the gouges might be the result of more distant seismic events (e.g., the Verona earthquake). Based on structural features and the presence of shattered and pulverized rocks in other sites along it (i.e., at Borcola Pass), the Schio-Vicenza Fault is the most probable source of the earthquakes which produced gouges and cataclasites present in the Euganean Hills.

DATA AVAILABILITY STATEMENT

The original contributions presented in the study are included in the article/**Supplementary Material**, further inquiries can be directed to the corresponding author.

REFERENCES

Altamimi, Z., Rebischung, P., Métivier, L., and Collilieux, X. (2016). ITRF2014: a new release of the International Terrestrial Reference Frame modeling nonlinear station motions. *J. Geophys. Res. Solid Earth* 121 (8), 6109–6131. doi:10.1002/2016jb013098

Anderlini, L., Serpelloni, E., Tolomei, C., De Martini, P. M., Pezzi, G., Gualandi, A., et al. (2020). New insights into active teconics and seismogenici potential of the Italian Southern Alps from vertical geodetic velocities. *EGU Earth Pub.* 11, 1681–1698. doi:10.5194/se-11-1681-2020

Antonelli, R., Barbieri, G., Dal Piaz, G. V., Dal Pra, A., De Zanche, V., Grandesso, P., et al. (1990). *Carta geologica del veneto 1:250000 e relative note illustrative.* Editor Selca (Firenze, Italy: Venezia), 31.

ETHICS STATEMENT

Written informed consent was obtained from the individual(s) for the publication of any potentially identifiable images or data included in this article.

AUTHOR CONTRIBUTIONS

FUNDING

ACKNOWLEDGMENTS

SUPPLEMENTARY MATERIAL

The Supplementary Material for this article can be found online at: https://www.frontiersin.org/articles/10.3389/feart.2020.586897/full#supplementary-material.

ARPAV (2005). ARPAV (osservatorio regionale suolo). Carta dei suoli del Veneto, scala 1, 250,000.

ASTM D4543-19 (2005). Standard practices for preparing rock core as cylindrical test specimens and verifying conformance to dimensional and shape tolerances.

ASTM D6913/D6913M-17 (2005). Standard Test Methods for Particle-Size Distribution (Gradation) of Soils Using Sieve Analysis.

ASTM D2487-17 (2005). Standard Practice for Classification of Soils for Engineering Purposes (Unified Soil Classification System).

ASTM D4318-17e1 (2005). Standard Test Methods for Liquid Limit, Plastic Limit, and plasticity Index of soils.

ASTM D6467-13e1 (2005). Standard Test Method for Torsional Ring Shear Test to Determine Drained Residual Shear Strength of Cohesive Soils.

ASTM D7928-17 (2005). Standard Test Method for Particle-Size Distribution (Gradation) of Fine-Grained Soils Using the Sedimentation (Hydrometer) Analysis.

Astolfi, G. and Colombara, F. (2003). *La geologia dei Colli Euganei*. 2nd Edn. Treviso, Italy: Canova, 240.

Bartoli, O., Meli, S., Bergomi, M. A., Sassi, R., Magaraci, D., and Liu, D.-Y. (2015). Geochemistry and zircon U-Pb geochronology of magmatic enclaves in trachytes from the Euganean Hills (NE Italy): further constraints on Oligocene magmatism in the eastern Southern Alps. *Eur. J. Mineral.* 27, 161–174. doi:10.1127/ejm/2015/0027-2425

Basili, R., Kastelic, V., Demircioglu, M. B., Garcia Moreno, D., Nemser, E. S., Petricca, P., et al. (2013). EDSF. The European database of seismogenic faults (EDSF) compiled in the framework of the project SHARE. http://diss.rm.ingv.it/share-edsf/. doi:10.6092/INGV.IT-SHARE-EDSF

Benà, E., Martin, S., Marzoli, A., Mazzoli, C., Sassi, R., and Zattin, M. (2019). "Apatite (U-Th)/He thermochronometry from trachytes and latites of the Euganean Hills and their exhumation history," in Abstract book of the 2019 SIMP-SGI-SOGEI Congress. Roma, Italy: Geological Society of Italym, 315.

Billi, A., Salvini, F., and Storti, F. (2003). The damage zone-fault core transition in carbonate rocks: implications for fault growth, structure and permeability. *J. Struct. Geol.* 25, 1779–1794. doi:10.1016/s0191-8141(03)00037-3

Billi, A. and Storti, F. (2004). Fractal distribution of particle size in carbonate cataclastic rocks from the core of a regional strike-slip fault zone. *Tectonophysics* 384, 115–128. doi:10.1016/j.tecto.2004.03.015

Brancolini, G., Civile, D., Donda, F., Tosi, L., Zecchin, M., Volpi, V., et al. (2019). New insights from the Adria plate geodynamics from the northern Adriatic perspective. *Mar. Petrol. Geol.* 109, 687–697. doi:10.1016/j.marpetgeo.2019.06.049

Brune, J. (2001). Fault normal dynamic loading and unloading: an explanation for non-gouge rock powder and lack of fault-parallel shear bands along the San Andreas Fault. *Eos Trans. AGU.* 82, 47.

Burrato, P., Poli, M. E., Vannoli, P., Zanferrari, A., Basili, R., and Galadini, F. (2008). Sources of Mw 5+ earthquakes in northeastern Italy and western Slovenia: an updated view based on geological and seismological evidence. *Tectonophysics* 453, 157–176. doi:10.1016/j.tecto.2007.07.009

Carminati, E., Doglioni, C., and Scricca, D. (2003). Apennines subduction-related subsidence of Venice (Italy). *Geophys. Res. Lett.* 30, 1717. doi:10.1029/2003gl017001

Carminati, E., Scrocca, D., and Doglioni, C. (2010). Compaction-induced stress variations with depth in an active anticline: northern Apennines, Italy. *J. Geophys. Res.* 115, B02401. 10.1029/2009JB006395

Castellarin, A., Vai, G. B., and Cantelli, L. (2006). The alpine evolution of the Southern Alps around the Giudicarie faults: a late Cretaceous to early Eocene transfer zone. *Tectonophysics* 414, 203–223. doi:10.1016/j.tecto.2005.10.019

Castiglioni, G. B. (1982a). "Abbozzo di una carta dell'antica idrografia nella pianura tra Vicenza e Padova," in *Scritti in onore di Aldo sestini*. Firenze: Società di Studi Geografici 183–197.

Castiglioni, G. B. (1982b). Questioni aperte circa l'antico percorso del Brenta nei pressi di Padova. *Atti. e. Mem. Accad. Patav.* 94 (1981–1982), 159–170. Padova, Italy: Soc. Coop. Tip. tav, 1.

Castiglioni, G. B. and Pellegrini, G. B. (2001). Note illustrative della Carta geomorfologica della Pianura padana. *Suppl. Geogr. Fis. Dinam. Quat.* 4, 208.

Castiglioni, G. B., Girardi, A., and Rodolfi, G. (1987). Le tracce degli antichi percorsi del Brenta per Montà e Arcella nei pressi di Padova: studio geomorfologico. *Mem. Sci. Geol.* 39, 129–149.

Cenni, N., Mantovani, E., Baldi, P., and Viti, M. (2012). Present kinematics of Central and Northern Italy from continuous GPS measurements. *J. Geodyn.* 58, 62–72. doi:10.1016/j.jog.2012.02.004

Cenni, N., Viti, M., Baldi, P., Mantovani, E., Bacchetti, M., and Vannucchi, A. (2013). Present vertical movements in central and northern Italy from GPS data: possible role of natural and anthropogenic causes. *J. Geodyn.* 71, 74–85. doi:10.1016/j.jog.2013.07.004

Chunga, K., Livio, F., Michetti, A. M., and Serva, L. (2007). Synsedimentary deformation of Pleistocene glaciolacustrine deposits in the Albese con Cassano Area (Southern Alps, Northern Italy), and possible implications for paleoseismicity. *Sediment. Geol.* 196 (1–4), 59–80. doi:10.1016/j.sedgeo.2006.08.010

Cook, N. G. W. (1965). The failure of rock. *Int. J. Rock Mech. Min. Sci. Geomech. Abstr.* 2 (4), 389–403. doi:10.1016/0148-9062(65)90004-5

Corbau, C., Simeoni, U., Zoccarato, C., Mantovani, G., and Teatini, P. (2019). Coupling land use evolution and subsidence in the Po Delta, Italy: revising the past occurrence and prospecting the future management challenges. *Sci. Total Environ.* 654, 1196–1208. doi:10.1016/j.scitotenv.2018.11.104

Cucato, M., De Vecchi, G. P., Miola, A., Monopoli, B., Piovan, S., Pola, M., et al. (2011). *Carta geologica D'italia—Padova sud—foglio, 147, 1:50000*. Firenze, Italy: APAT, Dipartimento difesa del suoloServizio geologico d'Italia.

Cucato, M., De Vecchi, G. P., Mozzi, P., Abbà, T., Paiero, G., and Sedea, R. (Eds.) (2012). Note illustrative della carta geologica D'italia alla Scala 1, 50,000, Foglio 147 Padova sud. ISPRA, 215.

D'Agostino, N., Avallone, A., Cheloni, D., D'Anastasio, E., Mantenuto, S., and Selvaggi, G. (Eds.) (2008). Active tectonics of the Adriatic region from GPS and earthquake slip vectors, *J. Geophys. Res.* 113, B12413. doi:10.1029/2008JB005860

De Marchi, L. (1935). Idrografia ed evoluzione morfologica.dei colli euganei. *Atti e Mem. R. Acc. SS.LL.AA. Padova* 1, 21–26.

De Marchi, L. (1905). L'idrografia dei Colli Euganean nei suoi rapporti colla geologia e la morfologia della regione. *Mem. Ist. Ven. SS.LL.AA* 27, 1–76.

De Zigno, A. (1861). Cenni sulla costituzione geologica dei Monti Euganean. *Riv Periodica dei lavori della I.R. Acc. SS.LL.AA Padova* 9, 93–108, Padova: G.B. Randi e Comp.

Dieni, I. and Proto Decima, F. (1970). Documentazione paleontologica dell'età oligocenica inferiore del vulcanismo euganeo. Atti e Mem. Acc. Patav. SS.LL.AA. Cl. Sc. Mat. Nat. 82, 321–360.

Doan, M.-L., and d'Hour, V. (2012). Effect of initial damage on rock pulverization along faults. *J. Struct. Geol.* 45, 113–124. doi:10.1016/j.jsg.2012.05.006

Doglioni, C. (1992a). Relationships between mesozoic extention tectonics, stratigraphy and alpine inversion in the southern Alps, eclogae geol. *Helv* 85 (1), 105–126.

Doglioni, C. (1992b). "The Venetian Alps thrust belt," in *Thrust Tectonics*. Editor K. R. McKlay (London: Chapman and Hall), 319–324.

Doglioni, C. (1993). Some remarks on the origin of foredeeps. *Tectonophysics* 228 (1–2), 1–20. doi:10.1016/0040-1951(93)90211-2

Dor, O., Ben-Zion, Y., and Rockwell, T. K. (2006). Pulverized rocks in the mojave section of the san Andreas fault zone. *Earth Planet Sci. Lett.* 245, 642–654. doi:10.1016/j.epsl.2006.03.034

Fanetti, D., Anselmetti, F. S., Chapron, E., and Sturm, M. L. (2008). Megaturbidite deposits in the Holocene basin fill of lake Como (southern Alps, Italy). *Palaeogeogr. Palaeoclimatol. Palaeoecol.* 259, 323–340. doi:10.1016/j.palaeo.2007.10.014

Fantoni, R. and Franciosi, R. (2010). Tectono-sedimentary setting of the Po Plain and Adriatic foreland. *Rendiconti Lincei.* 21, 197–209. doi:10.1007/s12210-010-0102-4

Ferrari, S., Peresani, M., and Perrone, R. (2009). Siti Mesolitici nella Valle di Mondonego (Comuni di Arquà Petrarca e Galzignano). "Dinamiche insediative nel territorio dei Colli Euganean dal Paleolitico al Medioevo". *Este-Monselice*, 79–82.

Finetti, I. (1972). *Le condizioni geologiche della regione di Venezia alla luce di recenti indagini sismiche. Bollettino di Geofisica Teorica*. Editor Applicata 14, 275–290.

Fondriest, M., Aretusini, S., Di Toro, G., and Smith, S. A. F. (2015). Fracturing and rock pulverization along an exhumed seismogenic fault zone in dolostones: the Foiana Fault Zone (Southern Alps, Italy). *Tectonophysics* 654, 56–74. doi:10.1016/j.tecto.2015.04.015

Fondriest, M., Doan, M.-L., Aben, F., Fusseis, F., Mitchell, T. M., Voorn, M., et al. (2017). Static versus dynamic fracturing in shallow carbonate fault zones. *Earth Planet Sci. Lett.* 461, 8–19. doi:10.1016/j.epsl.2016.12.024

Fondriest, M., Smith, S. A. F., Di Toro, G., Zampieri, D., and Mittempergher, S. (2012). Fault zone structure and seismic slip localization in dolostones, an example from the Southern Alps, Italy. *J. Struct. Geol.* 45, 52–67. 10.1016/j.jsg.2012.06.014

Fontana, A., Mozzi, P., and Bondesan, A. (2010). Late pleistocene evolution of the Venetian-Friulian plain. *Rendiconti Lincei* 21 (Suppl. 1), 181–196. doi:10.1007/s12210-010-0093-1

Fontana, A., Mozzi, P., and Marchetti, M. (2014). Alluvial fans and megafans along the southern side of the Alps. *Sediment. Geol.* 301, 150–171. doi:10.1016/j.sedgeo.2013.09.003

Galadini, F., Poli, M. E., and Zanferrari, A. (2005). Seismogenic sources potentially responsible for earthquakes with M ≥6 in the eastern Southern Alps (Thiene—Udine sector, NE Italy). *Geophys. J. Int.* 161, 739–762. doi:10.1111/j.1365-246x.2005.02571.x

Galadini, F., Poli, M. E., and Zanferrari, A. (2004). A Seismogenic sources potentially responsible for earthquakes with M ≥6 in the eastern Southern Alps (Thiene—udine sector, NE Italy). *Geophys. J. Int.* 161 (3), 739–762. 10.1111/j.1365-246X.2005.02571.x

Ghielmi, M., Minervini, M., Nini, C., and Rogledi, S. M. (2013). Late Miocene-Middle Pleistocene sequences in the Po Plain—northern

Adriatic Sea (Italy): the stratigraphic record of modification phases affecting a complex foreland basin. *Mar. Petrol. Geol.* 42, 50–81. doi:10.1016/j.marpetgeo.2012.11.007

Govoni, A., Marchetti, A., De Gori, P., Di Bona, M., Lucente, F. P., Improta, L., et al. (2014). The 2012 Emilia seismic sequence (Northern Italy): imaging the thrust fault system by accurate aftershock location. *Tectonophysics* 622, 44–55. doi:10.1016/j.tecto.2014.02.013

Guerrieri, L., Baer, G., Hamiel, Y., Amit, R., Blumetti, A. M., Comerci, V., et al. (2010). InSAR data as a field guide for mapping minor earthquake surface ruptures: ground displacements along the Paganica Fault during the 6 April 2009 L'Aquila earthquake. *J. Geophys. Res.* 115, B12331. doi:10.1029/2010JB007579

Guidoboni, E., Comastri, A., and Boschi, E. (2005). The "exceptional" earthquake of 3 January 1117 in the Verona area (northern Italy): a critical time review and detection of two lost earthquakes (lower Germany and Tuscany). *J. Geophys. Res. Solid Earth* 110 (B12), B12309. 10.1029/2005JB003683

Guidoboni, E., Ferrari, G., Mariotti, D., Comastri, A., Tarabusi, G., Sgattoni, G., et al. (2018). CFTI5Med, Catalogo dei Forti Terremoti in Italia (461 a.C.-1997) e nell'area Mediterranea (760 a.C.-1500). Istituto Nazionale di Geofisica e Vulcanologia (INGV). 10.6092/ingv.it-cfti5

Guidoboni, E., Ferrari, G., Mariotti, D., Comastri, A., Tarabusi, G., and Valensise, G. (2007). CFTI4Med, catalogue of strong earthquakes in Italy (461 B.C.-1997) and mediterranean area (760 B.C.-1500). Available at: http://storing.ingv.it/cfti4med/ (Accessed January 2007).

Guidoni, E., and Soragni, U. (1997). "Lo spazio nelle città venete (1348–1509). Urbanistica e architettura, monumenti e piazze, decorazione e rappresentazione," in *Atti del I convegno di studio. Verona, Dicembre 14–16, 1995.* Roma: Edizioni Kappa.

Herring, T. A., King, R. W., Floyd, M. A., and McClusky, S. C. (2018a). GAMIT reference manual, GPS analysis at MIT, Release 10.7. Cambridge: Massachusetts institute of technology.

Herring, T. A., King, R. W., and McClusky, S. C. (2018b). Global kalman filter VLBI and GPS analysis program, GLOBK reference manual, Release 10.6. Cambridge: Massachusetts institute of technology.

Hoek, E. (1964). Fracture of anisotropic rock. *J. S. Afr. Inst. Min. Metall.* 64 (10), 501–518.

Hoek, E. and Brown, E. T. (1980). Empirical strength criterion for rock masses. *J. Geotech. Eng. Div.* 106 (GT9), 1013–1035.

Hoek, E., and Brown, E. T. (2018). The Hoek-Brown failure criterion and GSI—2018 edition. *J. Rock Mech. Geotech. Eng.* 11, 445–463. doi:10.1016/j.jrmge.2018.08.001

ISRM (1978). SM for determining tensile strength of rock materials.

ISRM (1983). Suggested method for determining the strength of rock materials in triaxial compression: revised version.

ISRM (1979). Suggested method for determining the uniaxial compressive strength and deformability of rock materials.

ISRM (2006). *The complete ISRM suggested methods for rock characterization, testing and monitoring.* Editors R. Ulusay and J.A. Hudson (Cham, New York: Springer), 1974–2006.

Ivy-Ochs, S., Martin, S., Campedel, P., Hippe, K., Alfimov, V., Vockenhuber, C., et al. (2017b). Geomorphology and age of the marocche di dro rock avalanches (Trentino, Italy). *Quat. Sci. Rev.* 169, 188–205. doi:10.1016/j.quascirev.2017.05.014

Ivy-Ochs, S., Martin, S., Campedel, P., Hippe, K., Vockenhuber, C., Carugati, G., et al. (2017a). "Viganò, A Geomorphology and age of large rock avalanches in Trentino (Italy): Castelpietra," in *Advancing culture of living with landslides. WLF 2017.* Editors M. Mikoš, V. Vilímek, Y. Yin, and K. Sassa (Cham, New York: Springer), 347–353. doi:10.1007/978-3-319-53483-1_41

Jenkyns, H. C. (2010). Geochemistry of oceanic anoxic events. *Geochem. Geophys. Geosyst.* 11, Q03004. doi:10.1029/2009GC002788

Labuz, J. F., and Lang, A. (2012). Mohr-Coulomb Failure Criterion. *Rock. Mech Rock Eng.* 45, 975–979. doi:10.1007/s00603-012-0281-7-2012

Lacy, L. L. (1997). Dynamic rock mechanics testing for optimized fracture designs. *Soc. Petrol. Eng.* doi:10.2118/38716-MS

Livani, M., Scrocca, D., Arecco, P., and Doglioni, C. (2018). Structural and stratigraphic control on salient and recess development along a thrust belt front: the Northern Apennines (Po Plain, Italy). *J. Geophys. Res. Solid Earth* 123, 4360–4387. doi:10.1002/2017JB015235

Livio, F. A., Berlusconi, A., Zerboni, A., Trombino, L., Sileo, G., Michetti, A. M., et al. (2014). Progressive offset and surface deformation along a seismogenic blind thrust in the Po Plain foredeep (Southern Alps, Northern Italy). *J. Geophys. Res. Solid Earth* 119 (10), 7701–7721. doi:10.1002/2014jb011112

Livio, F. A., Ferrario, M. F., Frigerio, C., Zerboni, A., and Michetti, A. M. (2020). Variable fault tip propagation rates affected by near-surface lithology and implications for fault displacement hazard assessment. *J. Struct. Geol.* 130, 103914. doi:10.1016/j.jsg.2019.103914

Livio, F. A., Michetti, A. M., Sileo, G., Zerboni, A., Trombino, L., Cremaschi, M., et al. (2009). Active fault-related folding in the epicentral area of the December 25, 1222. (Io1/4 IX MCS) Brescia earthquake (Northern Italy): seismotectonic implications. *Tectonophysics* 476, 320–335.

Lomb, N. R. (1976). Least-squares frequency analysis of unequally spaced data. *Astrophys. Space Sci.* 39, 447–462. doi:10.1007/bf00648343

Mantovani, E., Viti, M., Babbucci, D., Tamburelli, C., and Cenni, N. (2020). How and why the present tectonic setting in the Apennine belt has developed. *J. Geol. Soc.* 176, 1291–1302. doi:10.1144/jgs2018-175

Marcolongo, B. and Zaffanella, G. C. (1987). Evoluzione paleogeografica della Pianura veneta atesino-padana. *Athesia* 1, 31–56.

Martin, S., Campedel, P., Ivy-Ochs, S., Viganò, A., Alfimov, V., Vockenhuber, C., et al. (2014). Lavini di Marco (Trentino, Italy): 36Cl exposure dating of a polyphase rock avalanche. *Quat. Geochronol.* 19, 106–116. doi:10.1016/j.quageo.2013.08.003

Massari, F., and Medizza, F. (1973). Stratigrafia e paleogeografia del Campaniano-Maastrichtiano nelle Alpi Meridionali (con particolare riguardo agli hard grounds della Scaglia rossa veneta). *Mem. Ist. Geol. Miner. Univ. Padova* 28 (1971–73), 1–62.

Massari, F., Medizza, F., and Sedea, R. (1976). "Evoluzione geologica dell'area euganea tra il Giurese superiore e l'Oligocene inferiore," in *Il sistema idrotermale euganeo-berico e la geologia dei colli euganean.* Editor G. Piccoli (Mem Ist. Geol. Miner. Univ. Padova), 30 (1975–1977), 174–197.

McClintock, F. A., and Walsh, J. B. (1962). "Friction on Griffith cracks in rocks under pressure," in Proceedings of the 4th US National congress of applied mechanics, Berkeley, United States, June 18–21, 1962. (New York: American Society of Mechanical Engineers), 1015–1021.

Michetti, A. M., Giardina, F., Livio, F., Mueller, K., Serva, L., Sileo, G., et al. (2012). Active compressional tectonics, Quaternary capable faults, and the seismic landscape of the Po Plain (N Italy). *Ann. Geophys.* 55 (5), 969–1001. doi:10.4401/ag-5462

Mitchell, T. M., Ben-Zion, Y., and Shimamoto, T. (2011). Pulverized fault rocks and damage asymmetry along the Arima-Takatsuki Tectonic Line, Japan. *Earth Planet Sci. Lett.* 308, 284–297. doi:10.1016/j.epsl.2011.04.023

Morelli, C. (1951). Rilievo sperimentale gravimetrico-magnetico nell'avampaese dei colli euganean. *Ann. Geofisc.* 4, 355–367. doi:10.4401/ag-5918

Mozzi, P. (2001). "Geologia, geomorfologia e idrografia," in *I suoli dei colli euganean.* Editors A. Garlato and A. F. Ragazzi (Legnaro, PD: Veneto Agricoltura).

Mozzi, P., Ferrarese, F., and Fontana, A. (2013). Integrating digital elevation models and stratigraphic data for the reconstruction of the post-LGM unconformity in the Brenta alluvial megafan (North-eastern Italy). *Alp. Mediterr. Quat.* 26 (1), 41–54.

Mozzi, P., Piovan, S., Rossato, S., Cucato, M., Abbà, T., and Fontana, A. (2010). Palaeohydrography and early settlements in Padua (Italy). *Italian J. Quat. Sci.* 23 (2bis), 387–400.

Nicolis, E. (1898). Sugli antichi corsi del fiume Adige. Contribuzione alla conoscenza della costituzione della pianura veneta. *Boll. Soc. Geol. It.* 17 (1), 1–75.

Norinelli, A. (1963). Rilievo gravimetrico della zona di Padova. *Mem. Acc. Patav. SS.LL. AA., Cl. Sc. Mat. Nat.* 75, 189–202.

Pellegrini, G. B. (1988). Aspetti morfologici ed evidenze neotettoniche della Linea Schio-Vicenza. *Suppl. Geogr. Fis. Dinam. Quat.* 1, 69–82.

Pellegrini, G. B. (2006). "Tav. 69. Edifici vulcanici estinti: Colli Euganean," in *Atlante dei tipi geografici.* 338–339.

Pesci, A., Teza, G., Casula, G., Cenni, N., and Loddo, F. (2010). Non-permanent GPS data for regional-scale kinematics: reliable deformation rate before the 6 April, 2009, earthquake in the L'Aquila area. *Ann. Geophys.* 53 (2), 55–68. doi:10.4401/ag-4740

Piccoli, G., Bellati, R., Binotti, C., Lallo, E., Sedea, R., Dal Pra, A., et al. (1976). Il sistema idrotermale euganeo-berico e la geologia dei Colli Euganean. *Mem. Ist. Geol. Miner. Padova* 30, 266.

Piccoli, G., Sedea, R., Bellati, R., Di Lallo, E., Medizza, F., Girardi, A., et al. (1981). Note illustrative della carta geologica dei Colli Euganean alla scala 1: 25.000. *Mem. di Sci. Geol. Univ. Padova* 34 (1980–81), 523–566.

Piovan, S., Mozzi, P., and Stefani, C. (2010). Bronze age paleohydrography of the southern Venetian plain. *Geoarchaeology* 25 (1), 6–35. doi:10.1002/gea.20300

Piovan, S., Mozzi, P., and Zecchin, M. (2012). The interplay between adjacent Adige and Po alluvial systems and deltas in the late Holocene (Northern Italy). *Geomorphologie* 18 (4), 427–440. doi:10.4000/geomorphologie.10034

Pola, M., Ricciato, A., Fantoni, R., Fabbri, P., and Zampieri, D. (2014). Architecture of the western margin of the North Adriatic foreland:the Schio-Vicenza fault system. *It. J. Geosci.* 133 (2), 223–234. doi:10.3301/ijg.2014.04

Poli, M. E., Burrato, P., Galadini, F., and Zanferrari, A. (2008). Seismogenic sources responsi- ble for destructive earthquakes in north-eastern Italy. *Boll. Geofis. Teor. Appl.* 49, 301–313.

Priolo, E. (a cura di) (2007). Relazione 2008-OGS043-CRS006-SIRE. Regione Veneto - gestione della rete di controllo sismico, studio della sismicità regionale e ricerca sismologica a fini di protezione civile. Available at: https://www.researchgate.net/publication/269915668 (Accessed March 2007).

Proto Decima, F. and Sedea, R. (1970). Segnalazione di Oligocene marino nei colli euganean (Padova). *Acc. Naz. Lincei Rend. Cl. Sc. Fis. Mat. Nat.* 48, 156–163.

Reches, Z. and Dewers, T. (2005). Gouge formation by dynamic pulverization during earthquake rupture. *Earth Planet Sci. Lett.* 235, 361–374. doi:10.1016/j.epsl.2005.04.009

Reyer, E. (1877). *Die euganeen, Bau und Geshichte eines Vulcanes 1 carta geol. 1: 29.000*. Wien: Hölder, 95.

Rice, J. R., Sammis, C. G., and Parsons, R. (2005). Off-fault secondary failure induced by a dynamic slip pulse. *Bull. Seismol. Soc. Am.* 95, 109–134. doi:10.1785/0120030166

Riguzzi, F., Crespi, M., Devoti, R., Doglioni, C., Pietrantonio, G., and Pisani, A. R. (2013). Strain rate relaxation of normal and thrust faults in Italy. *Geophys. J. Int.* 195 (2), 815–820. doi:10.1093/gji/ggt304

Rossato, S., Carraro, A., Monegato, G., Mozzi, P., and Tateo, F. (2018). Glacial dynamics in pre-Alpine narrow valleys during the last glacial maximum inferred by lowland fluvial records (northeast Italy). *Earth Surf. Dynam.* 6, 809–828. doi:10.5194/esurf-6-809-2018

Rossato, S., and Mozzi, P. (2016). Inferring LGM sedimentary and climatic changes in the southern Eastern Alps foreland through the analysis of a 14C ages database (Brenta megafan, Italy). *Quat. Sci. Rev.* 148, 115–127. doi:10.1016/j.quascirev.2016.07.013

Rossi, B., Thévenard, F., Fantin, M., and Giusberti, L. (2002). Late cretaceous plants from the Bonarelli level of the Venetian Alps, northeastern Italy. *Cretac. Res.* 23, 671–685. doi:10.1006/cres.2002.1026

Rovida, A., Locati, M., Camassi, R., Lolli, B., and Gasperini, P. (2020). The Italian earthquake catalogue CPTI15. *Bull. Earthq. Eng.* 18 (7), 2953–2984. doi:10.1007/s10518-020-00818-y

Rovida, A.N., Locati, M., Camassi, R.D., Lolli, B., and Gasperini, P. (Editors) (2016). CPTI15, the 2015 version of the Parametric Catalogue of Italian Earthquakes. Rome, Italy: Istituto Nazionale di Geofisica e Vulcanologia. doi:10.6092/INGV.ITCPTI15

Scarascia, S., and Cassinis, R. (1997). Crustal structures in the central-eastern Alpine sector: a revision of the available DSS data. *Tectonophysics* 271, 157–188. doi:10.1016/s0040-1951(96)00206-5

Scardia, G., Festa, A., Monegato, G., and Galadini, F. (2015). Evidence for late Alpine tectonics in the Lake Garda area (northern Italy) and seismogenic implications. *Geol. Soc. Am. Bull.* 127, 113–130. doi:10.1130/B30990.1

Scargle, J. D. (1982). Studies in astronomical time series analysis. II - statistical aspects of spectral analysis of unevenly spaced data. *Astrophys. J.* 263, 835–853. doi:10.1086/160554

Schlarb, A. (1961). Morphologischen studien in den Euganeen. *Geogr. Hefte.* 37, 171–199.

Scholz, C. H. (2002). *The mechanics of earthquakes and faulting*. Cambridge: Cambridge University Press.

Schröckenfuchs, T., Bauer, H., Grasemann, B., and Decker, K. (2015). Rock pulverization and localization of a strike-slip fault zone in dolomite rocks (Salzach-Ennstal-Mariazell-Puchberg fault, Austria). *J. Struct. Geol.* 78, 67–85. doi:10.1016/j.jsg.2015.06.009

Serpelloni, E., Vannucci, G., Anderlini, L., and Bennett, R. A. (2016). Kinematics, seismotectonics and seismic potential of the eastern sector of the European Alps from GPS and seismic deformation data. *Tectonophysics* 688, 157–181. doi:10.1016/j.tecto.2016.09.026

Teza, G., Pesci, A., and Galgaro, A. (2008). Grid_strain and grid_strain3: software packages for strain field computation in 2D and 3D environments. *Comput. Geosci.* 34 (9), 1142–1153. doi:10.1016/j.cageo.2007.07.006

Torresan, F., Piccinini, L., Pola, M., Zampieri, D., and Paolo, F. (2020). 3D hydrogeological reconstruction of the fault-controlled euganean geothermal system (NE Italy). *Eng. Geol.* 274, 105740. doi:10.1016/j.enggeo.2020.105740

Vannoli, P., Burrato, P., and Valensise, G. (2015). The seismotectonics of the Po Plain (Northern Italy): tectonic diversity in a blind faulting domain. *Pure Appl. Geophys.* 172, 1105–1142. doi:10.1007/s00024-014-0873-0

Viganò, A., Scafidi, D., Martin, S., and Spallarossa, D. (2013). Structure and properties of the Adriatic crust in the central-eastern Southern Alps (Italy) from local earthquake tomography. *Terra. Nova.* 25, 504–512. doi:10.1111/ter.12067

Viganò, A., Scafidi, D., Ranalli, G., Martin, S., Della Vedova, B., and Spallarossa, D. (2015). Earthquake relocations, crustal rheology, and active deformation in the central-eastern Alps (N Italy). *Tectonophysics* 661, 81–98. doi:10.1016/j.tecto.2015.08.017

Viganò, A., Tumiati, S., Recchia, S., Martin, S., Marelli, M., and Rigon, R. (2011). Carbonate pseudotachylytes: evidence for seismic faulting along carbonate faults. *Terra. Nova* 23, 187–194. doi:10.1111/j.1365-3121.2011.00997.x

Viganò, A., Zampieri, D., Rossato, S., Martin, S., Selli, L., Prosser, G., et al. (2018). Past to present deformation of the central-eastern Southern Alps: from the foreland to the Giudicarie belt. *ISPRA. Field Trips Maps* 10, 2018. doi:10.3301/GFT.2018.01

Wells, D. L., and Coppersmith, K. J. (1994). New empirical relationships among magnitude, rupture length, rupture width, rupture area, and surface displacement. *Bull. Seismol. Soc. Am.* 84, 974–1002.

Wilson, B., Dewers, T., Reches, Z. E., and Brune, J. N. (2005). Particle size and energetics of gouge from earthquake rupture zones. *Nature* 434 749–752. doi:10.1038/nature03433

Zaia, A., Benvenuti, G., and Bon, M. (1989). Misure magnetotelluriche nella pianura veneta a sud-est di Padova. *Atti 8° conv. Annuale GNGTS* 2, 871–879.

Zampieri, D., and Massironi, M. (2007). Evolution of a poly-deformed relay zone between fault segments in the eastern Southern Alps, Italy. *Geol. Soc. Spec. Pub.* 290, 351–366. doi:10.1144/sp290.13

Zampieri, D., Massironi, M., Sedea, R., and Sparacino, V. (2003). Strike-slip contractional stepovers in the southern Alps (northeastern Italy). *Eclogae Geol. Helv.* 96 (1), 115–123. doi:10.1007/S00015-003-1070-9

Zanolla, C., Braitenberg, C., Ebbing, J., Bernabini, M., Bram, K., Gabriel, G., et al. (2006). New gravity maps of the Eastern Alps and significance for the crustal structures. *Tectonophysics* 414, 127–143. doi:10.1016/j.tecto.2005.10.012